

COVALENTLY SUPPORTED IMIDAZOLIUM SALTS IN CATALYSIS

DOI: <http://dx.medra.org/10.17374/targets.2021.24.347>

Vincenzo Campisciano, Carla Calabrese, Francesco Giacalone, Michelangelo Gruttadauria

Department of Biological, Chemical and Pharmaceutical Sciences and Technologies,

Università di Palermo, Viale delle Scienze, Ed. 17, 90128 Palermo, Italy

(e-mail: michelangelo.gruttadauria@unipa.it)

Abstract. *Synthesis and catalytic applications of supported imidazolium salts covalently linked to the proper support are described. As supports here we report, among others, the use of amorphous and mesoporous silica, polyhedral oligomeric silsesquioxanes, magnetic-based silica, polystyrenes, halloysite nanotubes, carbon nanoforms such as fullerenes, carbon nanotubes, carbon nanohorns, graphene. The catalytic applications have been divided into two main sections, metal-free based and metal-based reactions.*

Contents

1. Introduction

2. Supported imidazolium salts as metal-free heterogeneous catalysts

3. Supported imidazolium salts as metal-based heterogeneous catalysts

4. Conclusions

Acknowledgement

References

1. Introduction

The aim of the present contribution is to provide an overview of the use of supported imidazolium salts for the production of heterogeneous catalysts applied in different organic transformations. Due to the large number of examples reported in literature, this chapter is far from constituting a comprehensive collection but only a few selected examples, in which imidazolium salts were covalently incorporated in the structure of different catalytic systems, were reported to provide a quick survey of this topic. The list of support materials used for the covalent immobilisation of imidazolium salts is long and includes both amorphous and mesoporous silica SBA-15, periodic mesoporous organosilica (PMO), polyhedral oligomeric silsesquioxanes (POSS), magnetic Fe₃O₄- and polystyrene-based supports, carbon nanoforms (CNFs), and halloysite nanotubes, among others. Furthermore, imidazolium-based ionic liquids (ILs) with polymerisable moieties were also used to produce heterogeneous catalysts without the need of a support material. The simple radical polymerisation of such type of polymerisable ILs afforded poly-ionic liquids (PILs), when only ILs-type monomers were used, or heterogeneous ionic copolymeric networks, when in addition to ILs different types of monomers were used. Here, we discuss about the use of these materials for selected metal-free catalysed transformations (cycloaddition of CO₂ to epoxides, Michael addition, transesterification, Knoevenagel reaction) and selected metal-catalysed reactions (Suzuki, Heck, hydrogenation, oxidation of alcohols, hydrosilylation of alkynes, etc.). The discussed hybrid systems were applied both as catalytic materials in which imidazolium salt moieties acted as catalysts themselves and as supports for metal species where, in this case, imidazolium salts played a central role in the stabilisation of the metal centres.

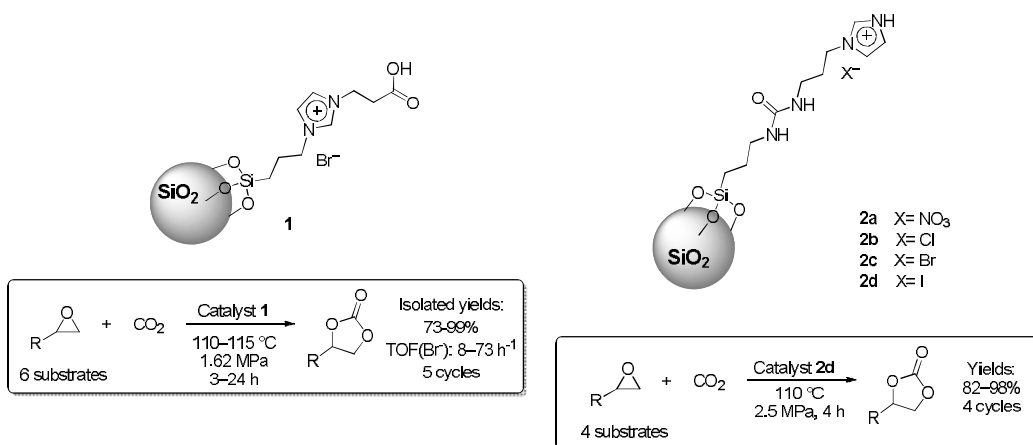
2. Supported imidazolium salts as metal-free heterogeneous catalysts

Imidazolium salts are one of the most investigated active species for the design of heterogeneous catalysts for the conversion of CO₂ by reaction with epoxides to produce cyclic carbonates. In this context, several metal-free catalytic materials have been prepared through the covalent grafting of imidazolium-based functionalities onto different solid supports such as amorphous or mesostructured silica, polymeric matrices and, most recently, carbon nanostructures.

The covalent functionalisation of silica surfaces with imidazolium moieties has been widely reported through condensation reactions between silanol groups of the support and a selected imidazolium-based organo-silane. By following this approach, a series of imidazolium-based ionic liquids bearing carboxyl moieties was supported onto a silica gel¹ to be tested as heterogeneous catalysts. The activity of the obtained hybrids was studied by considering the effect on the imidazolium structures focusing on the nature of the anionic species (Cl⁻, Br⁻, I⁻) and on the reaction parameters. The synergistic effect of the carboxylic group

with the halide anions was evidenced by comparison with the analogous material based on imidazolium salt-functionalised with alkyl moieties. Then, in order to investigate the recyclability and the applicability of this type of catalyst, material **1**, based on imidazolium bromide salts modified with carboxyl units, was tested for deeper studies (Scheme 1). The solid was successfully used for five runs in the reaction between carbon dioxide and allyl glycidyl ether at 110 °C for 3 h with a CO₂ pressure of 0.8 MPa in the absence of solvents. Furthermore, the applicability of the catalysts was verified with other epoxides affording high yields and selectivity corresponding to TOF values ranging from 8-73 h⁻¹.

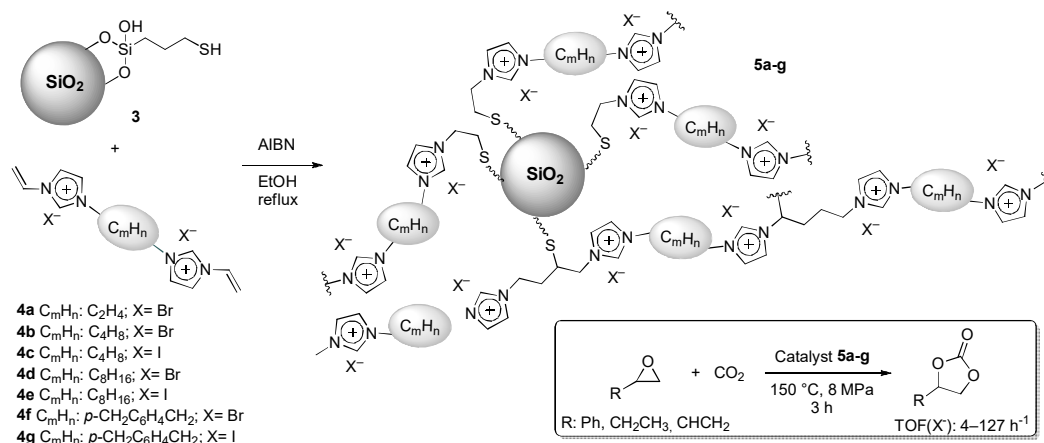
More recently, several zwitterionic imidazolium urea derivative frameworks bridged mesoporous hybrid silica materials were prepared by Arai and co-workers.² The materials displayed hydrogen bond donor capability and nucleophilicity **2a-d** (Scheme 1). The solid **2d** bearing iodide as anionic species emerged as the most active catalysts showing a high structural stability. Material **2d** was tested with different epoxides under solvent- and metal-free conditions. Moreover, the catalyst was separated by simple filtration and used four times without a significant loss of activity. This type of hybrid represents an alternative to Lewis acid activation and avoids the use of transition metal ions.



Scheme 1. Silica-supported imidazolium salts for the synthesis of cyclic carbonates.

A wide series of cross-linked imidazolium networks have been supported onto on thiol-functionalised silica supports **3** as heterogeneous catalysts based on chloride and bromide as nucleophilic active species.³ Some bis-vinylimidazolium salts having the *p*-xylyl as organic linker were grafted on **3** through a thiol-ene coupling reaction using 2,2'-azobisisobutyronitrile (AIBN) as radical initiator. The synthetic procedure led to a series of materials with good thermal stability and high catalytic loadings of about 3 mmol/g. These features are of paramount importance in terms of both catalyst recyclability and productivity. This study was performed under supercritical carbon dioxide at 150 °C, using a catalyst loading of 1 mol% to compare the activity of each solid with three substrates, such as propylene oxide, styrene oxide, and cyclohexene oxide. The catalytic tests were carried out in a high-throughput unit that allowed reactions to be performed simultaneously in parallel batch reactors. The best catalyst identified in this work was prepared by supporting onto SBA-15 a bis-imidazolium bromide salt with *p*-xylyl as organic linker between the imidazolium units. In order to further investigate the catalytic behaviour of this type of materials, an additional series of hybrids⁴ was designed by using bis-vinylimidazolium salts having different lengths and bulkiness of the organic linker connecting the two imidazolium units **4a-g**. The nature of the halide counterion was examined focusing on bromide and iodide organic salts (Scheme 2). The materials with iodide displayed higher activity in terms of conversion, productivity and turnover number compared to their counterparts with bromide as the counterion. A second catalytic trend was observed based on the specific organic linker: ranging from ethyl- to octyl alkyl chains the activity of the solids increased with the length of the linker. The material prepared by supporting a bis-vinylimidazolium iodide salt with the xylyl as the linker

5g was found to be the most active catalysts in the reaction between CO₂ and styrene oxide showing a turnover number of 237. The interesting features of this class of materials were also examined in terms of versatility with different substrates using catalytic loadings in the range 0.6-0.4 mol%, whereas the reusability of a selected catalyst at 0.1 mol% was verified for five consecutive cycles.



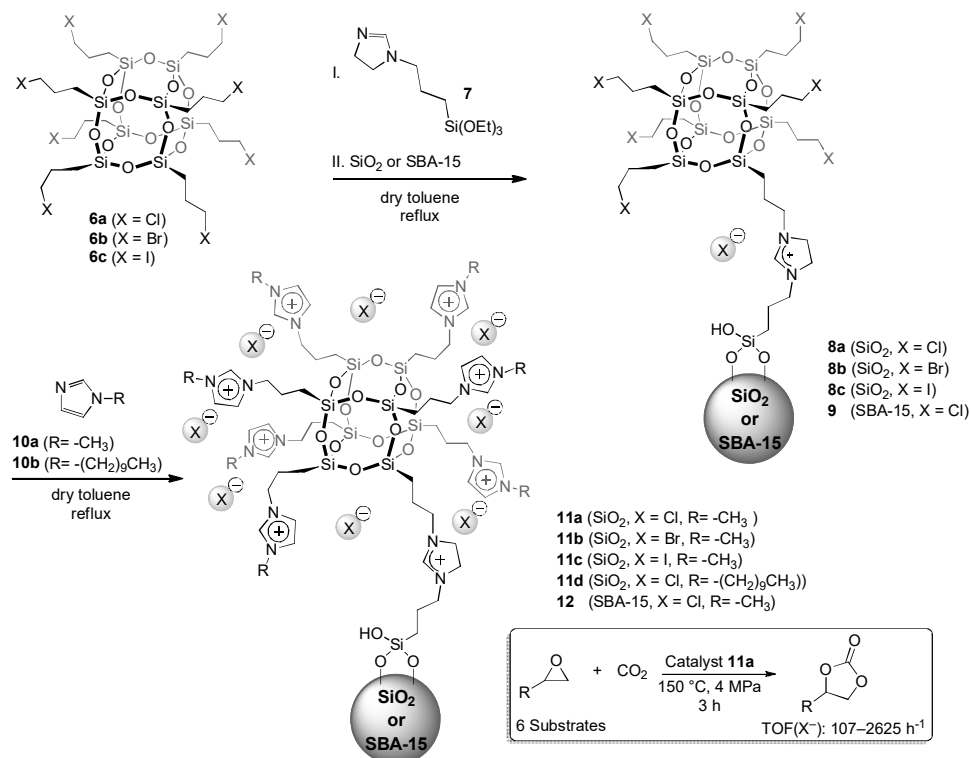
Scheme 2. Multilayered supported imidazolium salts for the synthesis of cyclic carbonates.

More recently, a novel series of hybrid materials based on silica-supported imidazolium modified polyhedral oligomeric silsesquioxanes (POSS-Imi) was prepared to be used as heterogeneous catalysts for the conversion of CO₂ and epoxides into cyclic carbonates under solvent- and metal-free reaction conditions.⁵ All the solids were easily prepared following tailored procedures (Scheme 3) designed to study the influence of the solid support (SiO₂ vs SBA-15) and the effect of both nucleophilic species (Cl⁻, Br⁻, I⁻) and imidazolium alkyl side chain length. POSS-supported catalyst were prepared from the reaction between POSS molecules **6a-c** and triethoxy-3-(2-imidazolyl)propylsilane **7**. The resulting POSS-based silanes were directly grafted onto two different supports to give materials **8a-c** (POSS-SiO₂, X=Cl, Br, I) and **9** (POSS-SBA15, X=Cl). These materials were in turn allowed to react with 1-methylimidazole **10a** allowing to obtain the corresponding **11a-c** (POSS-SiO₂) and **12** (POSS-SBA-15). In order to investigate the effect of the length of imidazolium alkyl side chain, a further hybrid was synthesised by reaction between **8a** and 1-decylimidazole **10b** to give catalyst **11d**. The proposed synthetic procedure has been developed to generate high local concentration spots of imidazolium active sites surrounding the POSS core. Such hybrid materials were recyclable as well as highly active toward the formation of cyclic carbonates even with the less reactive oxetane, showing higher performances in terms of turnover number, productivity and selectivity. High turnover numbers and productivity values up to 7875 and 740, respectively, have been recorded for the conversion of CO₂ into cyclic carbonates by using hybrid materials **6**.

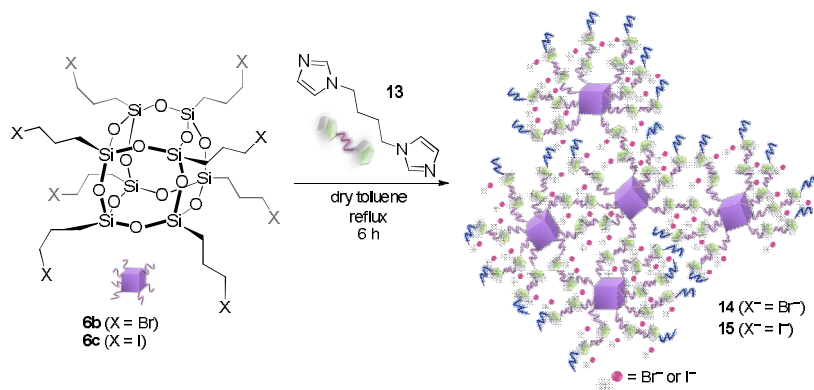
In the same year, two novel hybrid materials **14** and **15** based on highly cross-linked imidazolium networks were prepared from POSS molecular building blocks **6b-c** and 1,4-bis(*N*-imidazolyl)butane **13** depicted in Scheme 4 in order to be used as heterogeneous catalysts bearing different nucleophilic species (bromide and iodide).⁶ The catalysts were synthesised by following a simple one-pot procedure. The solids **14** and **15** were tested as the sole catalyst under metal- and solvent-free reaction conditions showing full selectivity toward the formation of cyclic carbonates. High TON and productivity values up to 5502 and 1081, respectively for glycidol at 100 °C and up to 4942 and 1122 for epichlorohydrin at 150 °C after 3 h, were reached. Such outstanding productivity values were conferred to the optimal organic/inorganic (*i.e.* imidazolium moiety/POSS support) weight ratio.

POSS nanocages were also employed for the design of imidazolium based catalytic systems by Koo and co-workers.⁷ They introduced a new methodology for the preparation of inorganic-organic hybrid ionogels and scaffolds through the cross-linking and solution extraction of POSS nanostructures modified

with vinyl-imidazolium or alkyl ammonium salts. The hybrid scaffolds with well-defined, interconnected mesopores were used as heterogeneous catalysts for the CO₂ conversion into several cyclic carbonates at 110 °C, 0.76 MPa for 10 h using an epoxide concentration 400 mM in MeCN. The obtained TOF values were calculated from the moles of ionic groups to be in the range of 16-21 h⁻¹. The materials recyclability exhibited good performance with minimal to no depreciation in catalytic conversion of ethylene oxide to ethylene carbonate, as the total catalytic conversion degree of decrease was only about 5%.

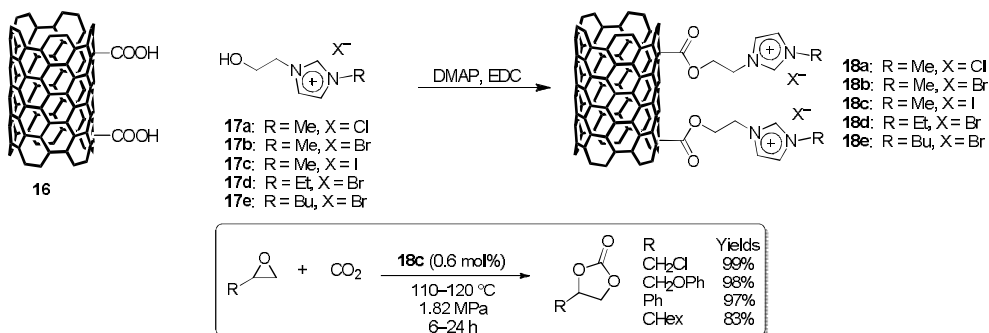


Scheme 3. Silica-supported imidazolium-based POSS for CO₂ conversion.



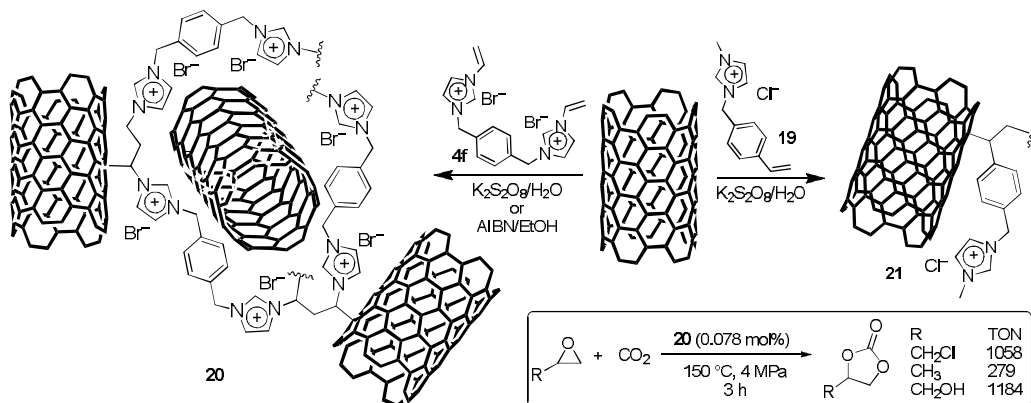
Scheme 4 Synthesis of imidazolium cross-linked POSS nanohybrids **14-15**.

In 2012 Park *et al.* used oxidized multi-walled carbon nanotubes (MWCNTs) **16** as support for the covalent grafting of a series of imidazolium-based ionic liquids **17a-e** with different anion and alkyl chain through esterification of the carboxylic groups present on the nanotubes (Scheme 5).⁸ All the prepared hybrid materials **18a-e** featured high loading in ionic liquid (1.59-2.40 mmol/g) and exhibited a good activity toward the cycloaddition of CO₂ to allyl glycidyl ether. Catalyst **18c** proved to be the most active and was applied for the conversion of a series of epoxides being easily recycled 5 times with just little loss in conversion.



Scheme 5. Imidazolium-modified carbon nanotubes **18a-e** for the synthesis of cyclic carbonates.

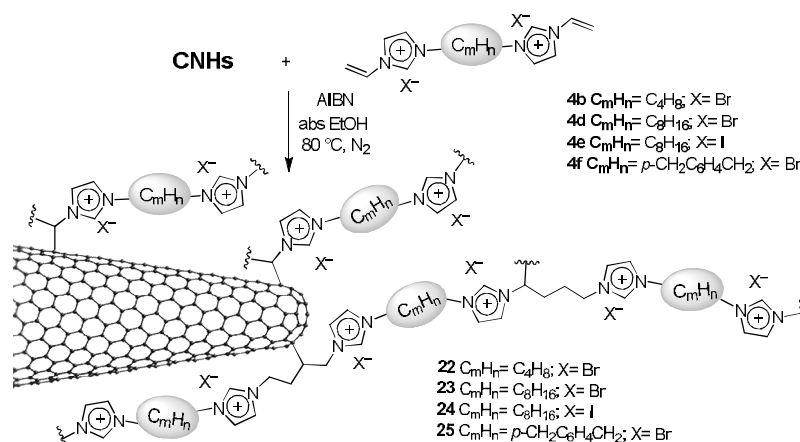
A further synthetic strategy for the immobilisation of imidazolium salts onto carbon nanotube surface lies in the direct radical polymerisation of bis-vinylimidazolium bromide **4f** and styryl imidazolium chloride **19** in the presence of single-walled carbon nanotubes (SWCNTs) gave rise to highly loaded SWCNT-polyimidazolium salts hybrids (Scheme 6).⁹ These hybrids were applied as catalysts in the conversion of carbon dioxide and a series of epoxides to the corresponding cyclic carbonates with TON of up to 1184 and TOF of 395 h⁻¹ with no need for additional Lewis acid co-catalyst. Although both catalysts displayed an analogue activity, **20** was easily reused for four runs with no deactivation whereas **21** was suffered significant leaching of polymer during the recycling.



Scheme 6. SWCNT-polyimidazolium salts hybrids **20** and **21** used as catalysts for the conversion of CO₂ and epoxides into cyclic carbonates.

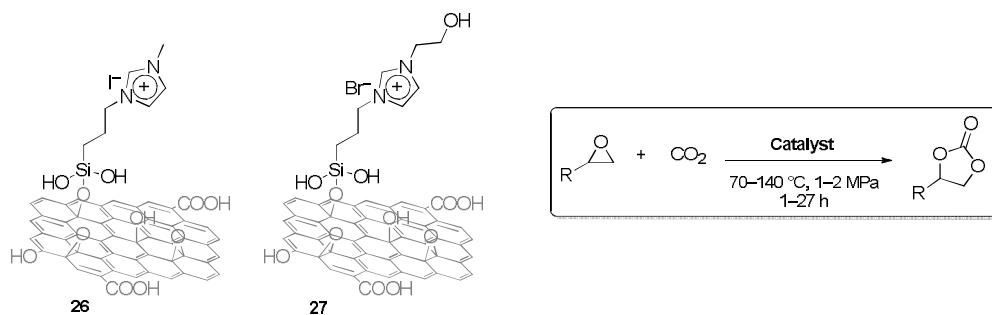
The importance of the nanocarbon support on the catalytic activity of the resulting hybrid was greatly evident when a series of polyimidazolium-functionalised carbon nanohorns (CNHs) were used for the conversion of CO₂ and epoxides into cyclic carbonates.¹⁰ These hybrid materials based on CNHs/cross-linked imidazolium salts were easily prepared using the direct radical polymerisation of

bis-vinylimidazolium salts **4b** and **4d-f** in the presence of pristine CNHs (Scheme 7). CNH-based catalysts **22-25** resulted extremely active materials showing an unprecedented increase of the catalytic activity from the first to the sixth cycle in the reaction with styrene oxide (catalyst 0.22 mol%, 4 MPa pressure of CO₂ at 150 °C for 3 h). Interestingly, a seventh cycle with epichlorohydrin showed an increased catalytic activity with respect to the first cycle with the same epoxide reaching TON of up to 2819. The same behaviour was not observed with the self-condensed polymer nor with the analogous SWCNT-based catalysts.⁹ This finding was ascribed to the higher percentage of porosity of the reused catalyst that was probably caused by an additional cross-linking of residual double bonds during the catalytic reaction.



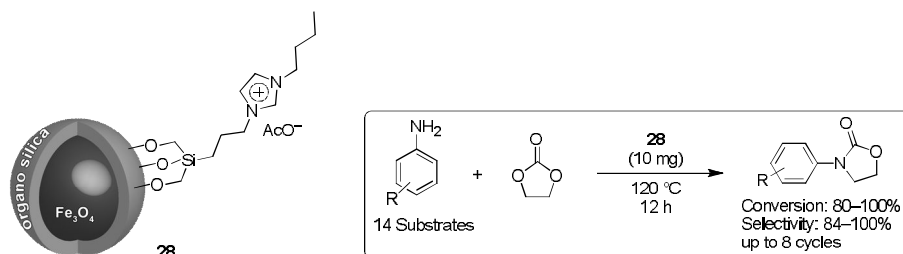
Scheme 7. Synthesis of imidazolium-functionalised CNHs **22-25**.

Li *et al.* reported the preparation of a series of imidazolium-based IL covalently supported onto the surface of GO which was tested as active and recyclable catalysts for the CO₂ cycloaddition to produce cyclic carbonates.¹¹ Hybrid **26** bearing iodide anionic species (Scheme 8) resulted the most performing catalyst (2 MPa pressure of CO₂ at 140 °C for 4 h) although 600 mg of modified-GO were used for 15 mL of epoxide. It is worth noting that the fundamental role played in the co-catalytic process by the residual hydroxyl groups of GO acting as hydrogen bond donors was highlighted, since their silylation resulted in a marked drop in the catalytic activity. The synergistic effect in accelerating the ring opening of epoxides by hydroxyl groups was further confirmed with the use of catalyst **27**, in which a hydroxyl functionalised IL was grafted onto GO (Scheme 8).¹² In this case, higher conversions of propylene oxide into the corresponding carbonate were obtained with 0.35 mol% of catalyst at 140 °C in 4 h showing the beneficial effect of hydroxyl-groups in the imidazolium tag. Furthermore, it was possible to recycle catalyst **27** up to seven times without loss of activity.



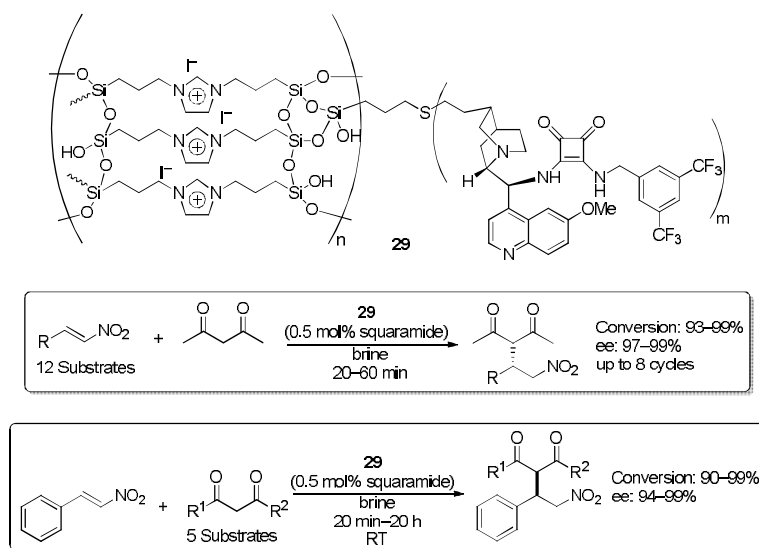
Scheme 8. Imidazolium-modified GO-based materials **26** and **27** for the synthesis of cyclic carbonates.

Acetate-based butylimidazolium ionic liquid has been immobilised onto silica-coated magnetic nanoparticles in order to obtain **28** as heterogeneous catalyst for the reaction of aniline and its derivatives with ethylene carbonate to form bioactive *N*-aryl oxazolidin-2-ones under metal-, ligand-, and solvent-free conditions (Scheme 9).¹³ Catalyst **28** was tested with a broad scope of substrates giving from high to quantitative conversion and selectivity values. The promising catalytic activity of **28** was ascribed to the efficient assemblies of hydrogen bond donors and acceptors allowing the cooperative activation of the substrates. Furthermore, this catalyst was easily recovered from the reaction mixture by using an external magnet. Its recyclability was successfully verified for eight consecutive runs without appreciable loss in catalytic efficiency.



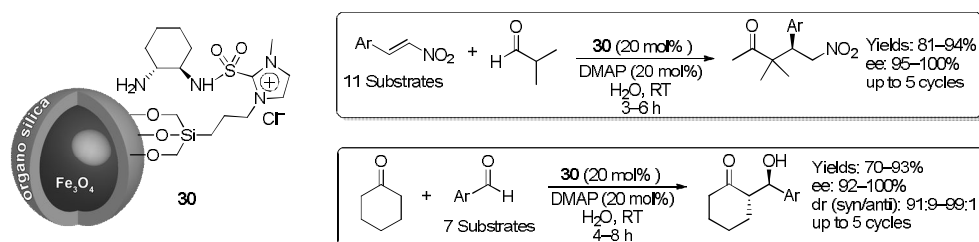
Scheme 9. Supported acetate-butylimidazolium catalyst **28** for the synthesis of *N*-aryl oxazolidin-2-ones.

Chiral cinchonine-substituted squaramide organocatalyst has been incorporated onto imidazolium-modified silica giving rise to **29** as bifunctional heterogeneous catalyst for asymmetric Michael additions (Scheme 10).¹⁴ Catalyst **29** has been prepared through post-grafting imidazolium-based silica supports with 3-mercaptopropyltrimethoxysilane followed by a thiol-ene reaction to anchor the chiral cinchona-based squaramide active centre. Catalyst **29** showed high catalytic activity and enantioselectivity in asymmetric Michael addition of 1,3-dicarbonyl compounds to nitroalkenes in brine. A synergistic effect of confined site-isolated squaramide species and the imidazolium phase-transfer function was observed on the whole catalytic performance. Furthermore, **29** has been easily recovered and reused at least eight times without loss of catalytic activity in the asymmetric Michael addition of acetylacetone to nitrostyrene.



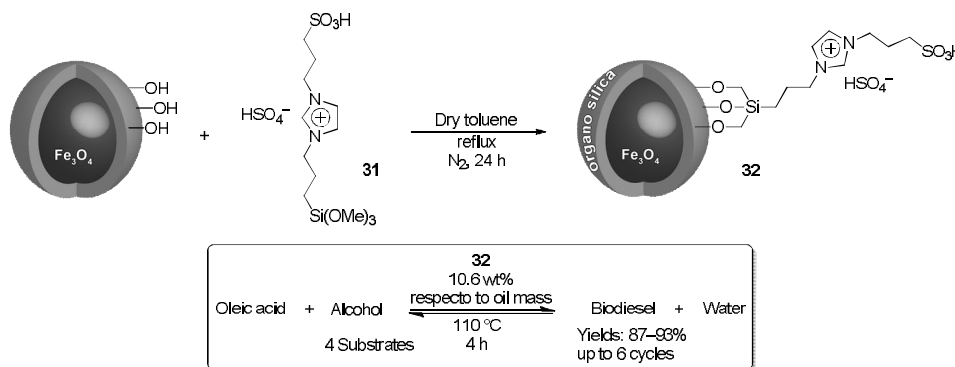
Scheme 10. Cinchonine-based squaramide onto imidazolium-based silica **29** for Michael additions.

In 2016, Xu and co-workers reported magnetic nanoparticles-supported catalyst **30** based on chiral aminocyclohexane combined with a sulfamide bearing an imidazolium functionality as linker between the active site and the core-shell structured silica support.¹⁵ The nano-sized catalyst **30** was used as heterogeneous catalyst in the asymmetric Michael addition and stereoselective aldol condensation (Scheme 11). By comparison of **30** with an ionic-free catalyst as counterpart, the authors claimed the role of the imidazolium moiety acting as a bridge between reactants and catalytic sites in water in the reaction of *trans*- β -nitrostyrene with isobutyraldehyde. Catalyst **30** was readily separated and recovered in the presence of an external magnet force, avoiding a more tedious work-up. The fresh catalyst **30** has been used for up to five times with no obvious decrease in catalytic efficiency in terms of stereoselectivity and product yield. Under optimised reaction conditions, the reaction scope for the asymmetric Michael addition was explored by varying the nitroolefins whether substituted by electron-donating groups or electron-withdrawing groups on the aromatic ring. High yield (>80%) and enantioselectivity (>95%) values were afforded at room temperature within 5 h. Furthermore, catalyst **30** was also used in the asymmetric aldol condensation of cyclohexanone and aromatic aldehydes.



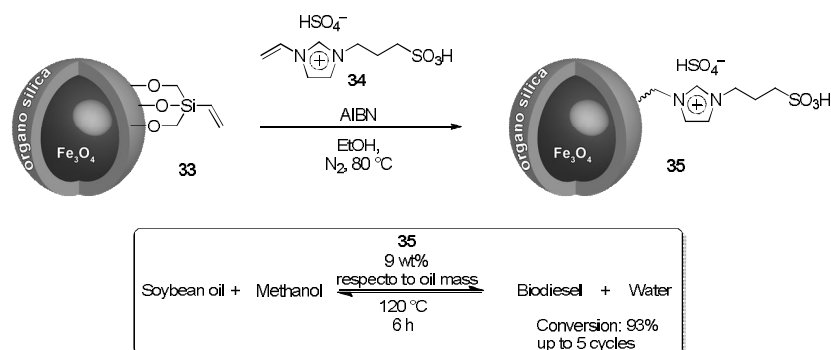
Scheme 11. Magnetic nanoparticles-supported catalyst **30** based on chiral aminocyclohexane combined with a sulfamide bearing an imidazolium functionality for asymmetric Michael and aldol reactions.

Another magnetic core-shell structured silica support was functionalised through condensation of imidazolium Brønsted acidic ionic liquid **31** allowing obtaining hybrid material **32** as heterogeneous catalyst for biodiesel production (Scheme 12).¹⁶ The catalyst exhibited a specific surface area of 175 m²/g and mesoporous channels in the outer silica shell. The catalytic activity of **32** was examined in the esterification of oleic acid with alcohols, at 110 °C affording biodiesel yields in the range 87-93% in 4 h. Such catalytic system could be easily recovered *via* magnetic separation and reused for up to six runs in the reaction between oleic acid and ethanol. The recyclability studies of **32** showed that the catalyst maintained good catalytic activity for six cycles, with a yield decrease from 93.5% to 87.4%. Such decrease in the catalytic performance was ascribed to a minor leaching of acidic protons or to the adsorption of reactant molecules on the active sites. Furthermore, the catalytic activity no longer decreased after five cycles.



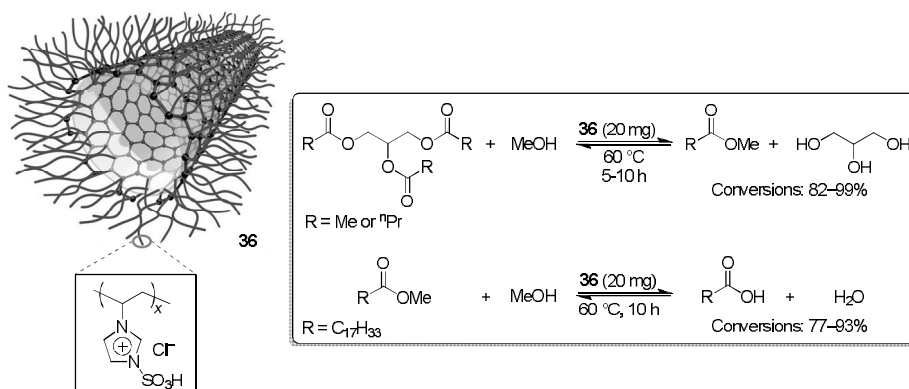
Scheme 12. Magnetic nanoparticles-supported catalyst **32** for biodiesel production.

More recently,¹⁷ a magnetic $\text{Fe}_3\text{O}_4/\text{SiO}_2$ composite based on iron oxides as the core and silica as the shell, was functionalised by condensation with 1-vinyltriethoxysilane. The resulting hybrid support **33** was in turn reacted through radical grafting copolymerisation of Brønsted acidic imidazolium salt **34** to afford hybrid material **35** (Scheme 13). The thus obtained **35** was used as catalyst for both transesterification of soybean oil and esterification of free fatty acids generally presented in low-cost oils. The transesterification of soybean oil with methanol to biodiesel was carried out at 120 °C for 6 h leading to the oil conversion of 93.3%. The catalyst was simply recovered magnetically and efficiently reused for five runs without significant loss in its activity.



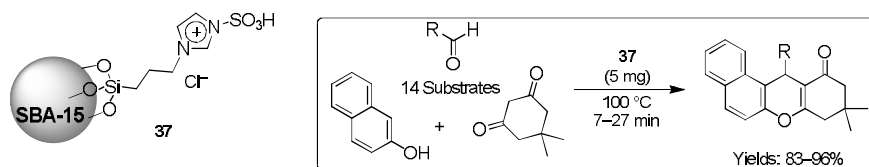
Scheme 13. Magnetic nanoparticles-supported catalyst **35** for biodiesel production.

Sulfonic acid imidazolium polymeric networks have been covalently grafted on multiwalled carbon nanotubes to give **36** as heterogeneous material for liquid phase transesterification of triglycerides with methanol and esterification of oleic acid with methanol (Scheme 14).¹⁸ The uniform distributions of polyimidazolium sulfonic coating over the outer surface of MWCNTs was able to promote both the access of reactants and the migration of reagents away from the catalyst. The reusability of **36** was investigated for the transesterification of glyceryl tributyrate and methanol. A six-cycle experiment was carried out at a low glyceryl tributyrate conversion level. In this case, the conversions of glyceryl tributyrate decreased from 52.4% to 40.9% after the six-cycle, indicating that the catalyst loses partial activity during the recycling processes. The elemental analysis revealed that in contrast to fresh catalysts **36** the recovered one showed a reduced $-\text{SO}_3\text{H}$ concentration from 1.46 to 0.96 mmol g^{-1} . This observation was attributed to the swollen of the polymer layer and subsequent partial cleavage of covalently linked polyimidazolium chains on CNTs.



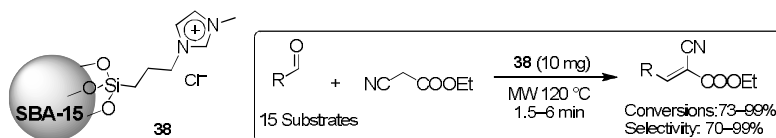
Scheme 14. Imidazolium-functionalised CNTs with sulfonic acids moieties **36** for the transesterification of triglycerides with methanol and esterification of oleic acid with methanol.

Silica-bonded imidazolium sulfonic acid chloride **37** has been prepared and utilised as heterogeneous nanocatalyst for the one-pot three-component condensation reaction of arylaldehydes with 2-naphthol and dimedone (5,5-dimethylcyclohexane-1,3-dione) to produce 12-aryl-8,9,10,12-tetrahydrobenzo[*a*]-xanthen-11-one derivatives (Scheme 15).¹⁹ In order to assess the versatility of **37**, the synthesis of tetrahydrobenzo[*a*]xanthen-11-ones was carried out by using different aromatic aldehydes with electron-donating or electron-withdrawing substituents. Under previously optimised reaction conditions, catalyst **37** was tested in the absence of solvent at 100 °C leading to the desired products in high yields (83-96%) and in short reaction times (7-27 min). The recyclability of **37** was investigated in the reaction of 2-naphthol with dimedone and 4-chlorobenzaldehyde for four cycles showing a decrease in the catalytic performances from the first to the fourth run in terms of yields (94-84%) and reaction times (12-19 min).



Scheme 15. Imidazolium sulfonic acid chloride grafted onto silica **37** for the synthesis of 12-aryl-8,9,10,12-tetrahydrobenzo[*a*]-xanthen-11-ones.

Imidazolium chloride moieties have been immobilised onto SBA-15 in order to obtain **38** as heterogeneous catalyst for Knoevenagel condensation (Scheme 16).²⁰ A broad scope of aromatic and heteroaromatic aldehydes were reacted with ethyl cyanoacetate by using **38** in solvent-free conditions through single mode microwave irradiation within short reaction times of 6 min. The catalyst was easily recovered by filtration and reused for three consecutive cycles without loss of its catalytic activity.

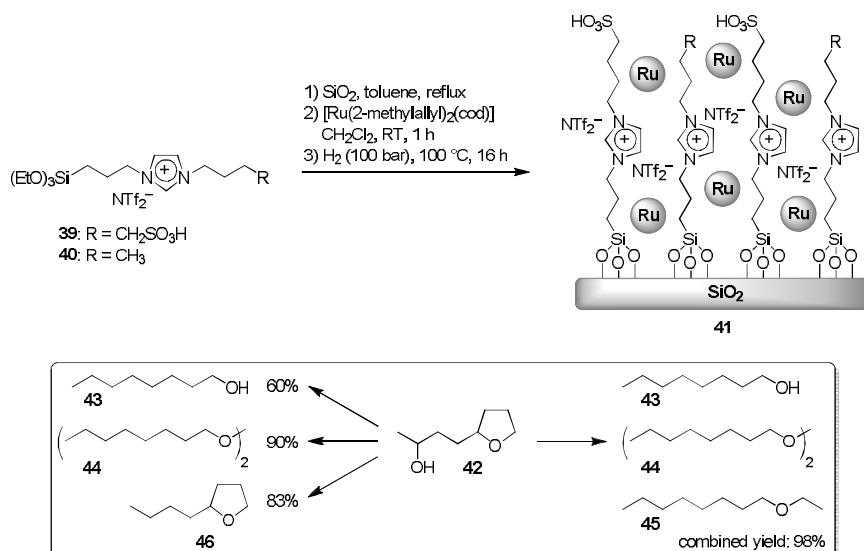


Scheme 16. Imidazolium-functionalised SBA-15 **38** as catalysts for Knoevenagel condensations.

3. Supported imidazolium salts as metal-based heterogeneous catalysts

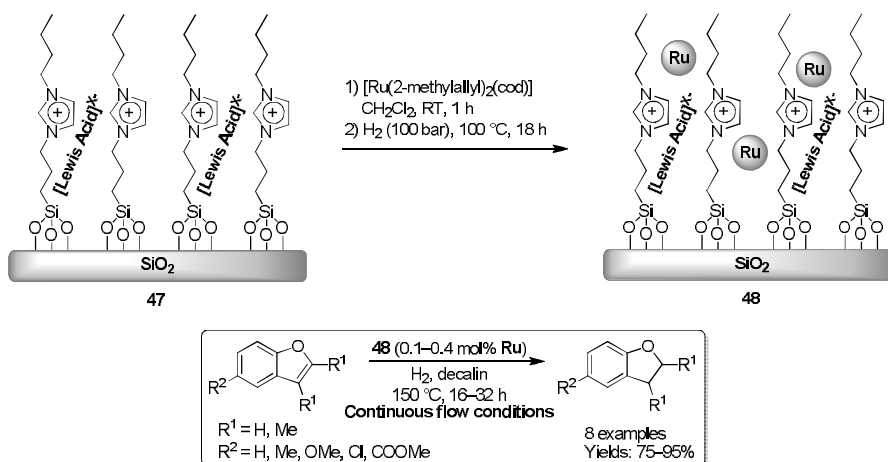
Leitner *et al.* designed a series of bifunctional catalysts based on an acid-functionalised IL immobilised onto silica acting as stabilisation medium for ruthenium nanoparticles (Ru NPs) with the aim to obtain highly active, selective and recyclable heterogeneous catalysts for the hydrogenolytic deoxygenation and ring opening of C₈- and C₉-substrates derived from furfural or 5-hydroxymethylfurfural and acetone (Scheme 17).²¹ The prepared catalytic materials, with the general structure **41** and with different acid loadings, were obtained by varying the ratio between a sulfonic acid-functionalised IL, [1-(4-sulfobutyl)-3-(3-triethoxysilylpropyl)imidazolium]NTf₂ **39**, and [1-butyl-3-(3-triethoxysilylpropyl)-imidazolium]NTf₂ **40** grafted onto SiO₂. Ru NPs precursor, in the form of an organometallic complex, was adsorbed onto the SiO₂-immobilised IL materials by means of their wet impregnation with a solution of [Ru(2-methylallyl)₂(cod)] (cod=cyclooctadiene) in dichloromethane, which caused a colour transition of the support materials from white to bright yellow. Upon evaporation of the solvent *in vacuo*, the impregnated SiO₂-IL was subjected to an atmosphere of H₂ (100 bar) at 100 °C for 16 h. Ru NPs formation was associated with a colour change of the catalytic materials from bright yellow to black. In the best catalytic conditions, when the catalyst with the higher acid loading was used for the hydrogenolysis of 4-(2-tetrahydrofuryl)-2-butanol **42**, a very high combined yield (98%) of 1-octanol **43**, 1,1-dioctylether **44**, and ethyloctylether **45** was achieved. The recycling of catalyst **41** for further two cycles showed that the reactivity profile was unchanged with only a slight decrease in activity (combined yield: 88%). Furthermore, the fine tuning of the reaction conditions, as well as the choice of the catalyst with the proper acidity,

allowed for the selective formation in good to excellent yields of 2-butyltetrahydrofuran **46**, 1-octanol **43**, or 1,1-dioctylether **44** from compound **42**.



Scheme 17. Preparation of materials **41** and their application in the deoxygenation of 4-(2-tetrahydrofuryl)-2-butanol **42**.

In another work, Leitner *et al.*, modified the structure of materials **41** by producing a Lewis acid-supported ionic liquid phase material (SILP-LA) **47**, in which the LA (mainly [ZnCl₄]²⁻) was present as counterion of the imidazolium moieties. Material **47** was used as support for Ru NPs to produce Ru@SILP-LA **48** (Scheme 18).²²

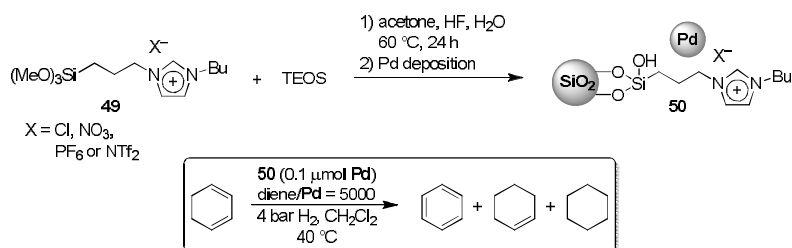


Scheme 18. Synthesis of material **48** and its application in the hydrogenation of benzofuran derivatives under continuous flow conditions.

Material **48** was used as selective catalyst for hydrogenation of benzofuran derivatives to dihydrobenzofurans under continuous flow conditions allowing the hydrogenation of O-containing

heteroaromatic rings while keeping the aromaticity of C6-rings intact. The catalytic system **48** was designed in such a way to bring metal and LA sites in close contact. Transmission electron microscopy (TEM) analysis and inductively coupled plasma atomic absorption spectroscopy (ICP-AAS) measurements revealed that both the dimension of Ru NPs (1.9 nm) and the LA and IL content remained unchanged in the reused material **48**, highlighting the high stability of this catalyst.

A sol-gel process in the presence of 1-*n*-butyl-3-(3-trimethoxysilylpropyl) imidazolium cation associated with hydrophilic and hydrophobic anions **49**, TEOS, in a H₂O-acetone mixture and aqueous HF was applied for the preparation of different organosilicas, which were decorated with palladium nanoparticles (Pd NPs) by sputtering deposition (Scheme 19).²³ Sputtering deposition allowed the generation of well-dispersed Pd NPs with similar sizes (1.8-2.1 nm) onto all the supports. Rutherford backscattering spectrometry (RBS) analysis was used to study the relative depth profile of Pd NPs in the different materials. Higher Pd concentration at the surface compared with the deeper regions of the supports with smaller pore diameters (containing hydrophilic ILs) was detected, whereas hybrid materials with the largest pore diameters (containing hydrophobic ILs) presented a more uniform distribution of Pd NPs. The catalysts **50** were tested in the selective hydrogenation of 1,3-cyclohexadiene. Since all the catalysts showed similar Pd NPs sizes, the differences in the catalytic activities were attributed to the nature of the IL layer. Indeed, IL hydrophobicity played a crucial role by controlling the diene access to NPs surface. The measured activities of the different catalysts, showed that materials containing hydrophobic PF₆⁻ and NTf₂⁻ anions were more active (3.03 and 2.82 s⁻¹, respectively) than the catalyst that did not possess IL (1.75 s⁻¹) that was more active than the catalysts containing the hydrophilic NO₃⁻ and Cl⁻ anions (0.96 and 0.86 s⁻¹, respectively).

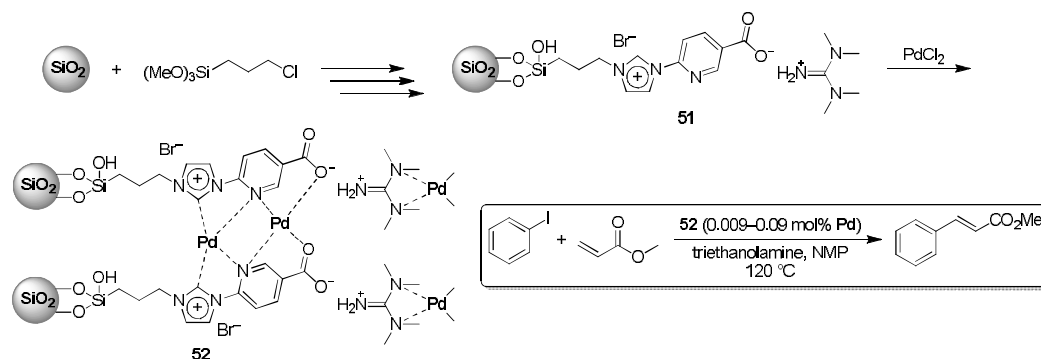


Scheme 19. Preparation of materials **50** and their use in the hydrogenation of 1,3-cyclohexadiene.

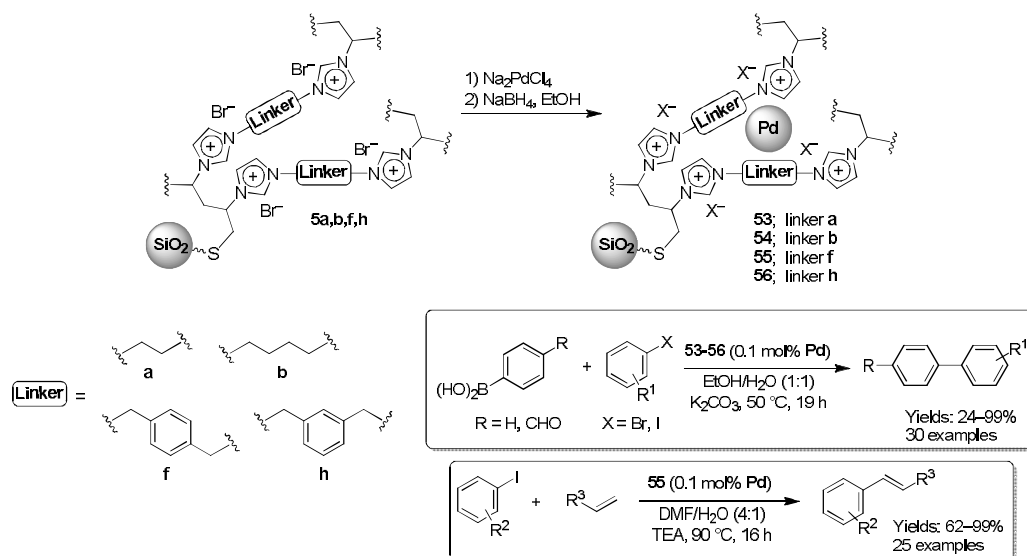
With the aim of obtaining a catalyst for the Heck reaction, a new bis-layered supported ionic liquid catalyst (SILCA) decorated with palladium was designed and produced.²⁴ The SILCA **51** consisted of a first IL layer (imidazolium bromide covalently grafted onto silica) on which a second layer, formed by pyridine-carboxylic acid balanced with tetramethylguanidinium (TMG) cation, was linked (Scheme 20). Palladium species in the Pd-SILCA system **52** were highly stabilised by means of different interactions involving IL, pyridine-carboxylic acid moiety, as well as the TMG cation. Very high turnover frequencies (TOFs) of 22,000 h⁻¹ were achieved in the Heck reaction of iodobenzene and methyl acrylate in which low Pd loadings (down to 0.009 mol%) were used. A “release and catch” mechanism was hypothesised where, at the end of the reaction, the TMG cation had the purpose to recapture all the Pd active species released during the catalytic process. Recycling tests of the catalyst used with a higher Pd loading (0.09 mol%) showed that it was possible to reuse this catalytic system up to 5 cycles before the activity started to decrease and a prolonged reaction time was needed to reach comparable conversion values.

A series of highly cross-linked imidazolium-based materials **5a,b,f** and **5h** were obtained according to the procedure reported in Scheme 2. Materials **5a,b,f** and **5h**, bearing different linkers (ethyl, butyl, *p*-xylyl, and *m*-xylyl), were used as supports for Pd NPs obtained by means of the exchange of bromide ions with tetrachloropalladate ions and reduction with sodium borohydride materials **53-56** (Scheme 21).²⁵ Owing to the high imidazolium loading, materials **5a,b,f** and **5h** were able to stabilise a great amount of the metal (10 wt%). Materials **53-56** showed good catalytic activity in the Suzuki reaction for the synthesis of several biphenyl compounds in high yields using a catalytic loading of 0.1 mol% of Pd at 50 °C in ethanol/water under batch conditions. Recycling tests (three cycles) under batch conditions were also carried out.

Furthermore, a flow apparatus in which, for the first time, the Pd-based catalyst and base (K_2CO_3) were placed in two different columns was assembled. Catalysts **53** and **54** were tested under flow conditions affording high yields of three different biaryls using a 0.1 mol% of Pd loading in ethanol. Recycling experiments proved the stability of catalysts **53** and **54** for four cycles achieving a turnover number (TON) of 3800. Under the flow conditions only 42 mg of catalyst were sufficient to produce up to 27 g of 4-bromotoluene, and a very low environmental factor (E-factor) was obtained. Catalyst **55** was also tested with a 0.1 mol% Pd loading in the Heck reaction between aryl iodides and alkenes (methyl acrylate, styrene derivatives, and methyl vinylketone) in DMF/ H_2O in the presence of triethylamine (TEA) at 90 °C.²⁶



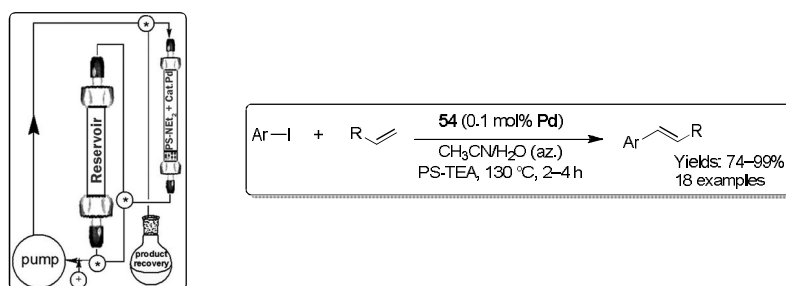
Scheme 20. Preparation of Pd-SILCA catalyst **52** and its use in the Heck reaction between iodobenzene and methyl acrylate.



Scheme 21. Synthetic route followed for the preparation of highly cross-linked imidazolium-based materials **53-56** and their application in the Suzuki and Heck reactions.

Catalyst **54** was also used for the development of an efficient continuous-flow approach in which the highly toxic DMF, usually used in the Heck reaction, was replaced with a greener, recoverable, and reusable medium consisting of acetonitrile/water azeotrope, allowing for reduction of waste.²⁷ The application of the flow technology ensured the fully reuse of both the catalyst **54** and the chosen heterogeneous base

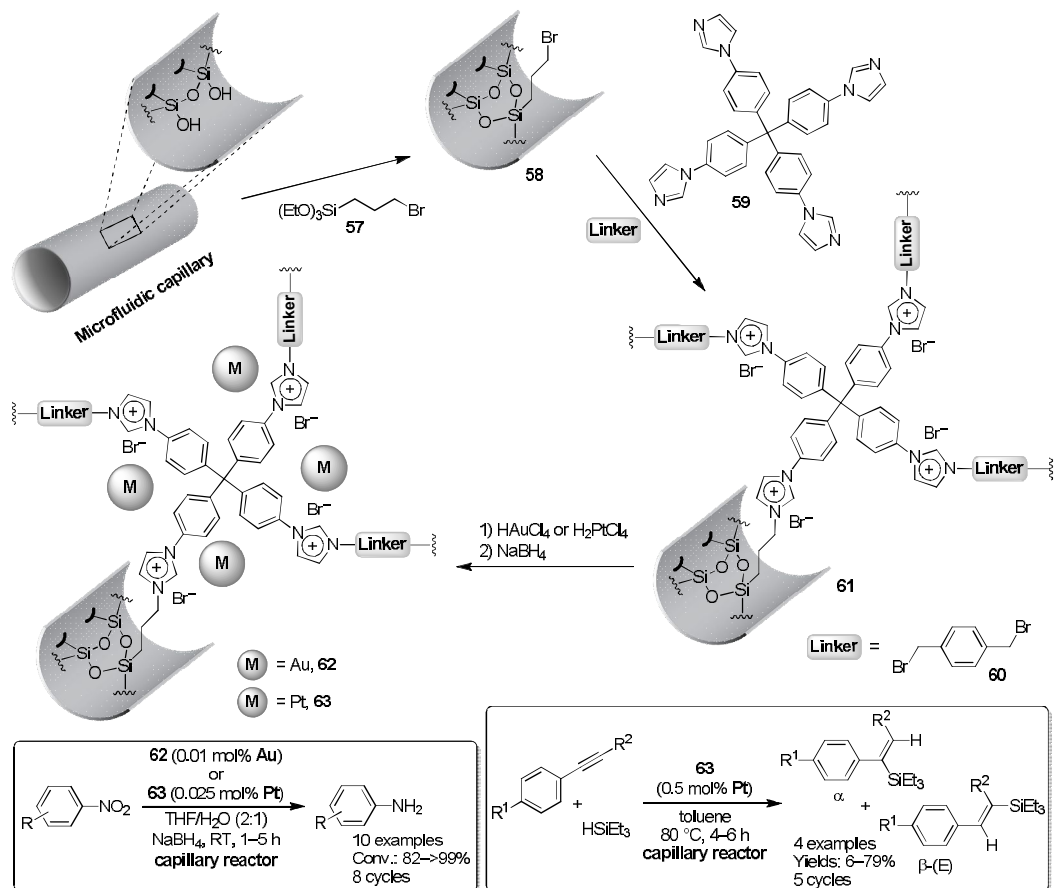
diethylaminomethyl-polystyrene (PS-TEA) for four cycles working at a 50 mmol scale per cycle (Scheme 22). In these conditions, extremely low E-factor values (2.3-5.0) and high yields (74-99%) of the desired products without the need of purification by means of chromatography and with very low residual palladium content (<5 ppm) were obtained.



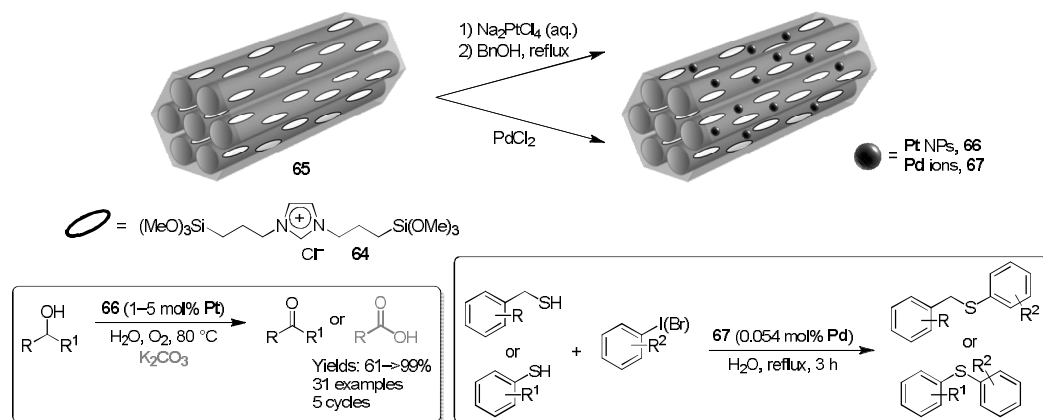
Scheme 22. Heck reaction catalysed by **54** under flow conditions.

A variety of imidazolium-based porous organic polymers were grafted along the inner surface of a fused-silica microfluidic capillary and used as supports for the immobilisation of gold (Au) and platinum nanoparticles (Pt NPs).²⁸ The procedure for the capillary coating involved the bromination of the inner surface of the capillary, previously subjected to a NaOH-induced hydroxylation process, by the treatment with (3-bromopropyl)triethoxysilane **57**, to afford system **58**. Subsequently, tetrakis[4-(1-imidazolyl)phenyl]methane **59** and different linkers (only 1,4-bis(bromomethyl)benzene linker **60** was shown in Scheme 23) were injected into the capillary using a syringe pump yielding systems **61** with different thickness of the porous organic layer depending on the precursor concentration. Au or Pt were immobilised onto support **61** by means of the ion exchange between bromide ions and AuCl_4^- and PtCl_6^{2-} , respectively, followed by reduction with sodium borohydride and formation of metal NPs stabilised within the porous channels of systems **62** and **63** (Scheme 23). The capillary coated **62** and **63** were assembled to obtain a catalytic microfluidic reactor for the reduction of nitrobenzene derivatives and hydrosilylation of phenylacetylene with triethylsilane. The catalytic microfluidic reactor showed significantly improved activity in comparison with the corresponding reactions carried out under batch conditions, possibly caused by the higher surface exposition of metal NPs when confined into the porous organic polymer layer inside the capillary. Moreover, systems **62** and **63** displayed good recyclability and stability in the investigated processes.

Periodic mesoporous organosilica (PMO) materials is a hybrid organic-inorganic porous silica containing organosilane bridges. The use of a dialkyl imidazolium bridge (1,3-bis(3-trimethoxysilylpropyl)imidazolium **64**, along with other silica precursors (tetramethyl (TMOS) or tetraethyl orthosilicate (TEOS)), and Pluronic P123 surfactant as the structure-directing agent, allowed to obtain IL-PMO material **65**, which was used as a suitable support for different metal species (Scheme 24). Both Pt NPs and Pd ions were immobilised onto IL-PMO material **65** for different purposes such as aerobic oxidation of alcohols in water and *S*-arylation couplings, respectively.²⁹ In the case of material **66**, both the preformation of Pt NPs supported onto IL-PMO hybrid material, as well as the choice of the proper reducing agent (benzyl alcohol rather than sodium borohydride) showed to be a fundamental factor to achieve good activity and selectivity in the oxidation of a wide variety of alcohols (Scheme 24). Furthermore, the presence of the imidazolium moiety in the IL-PMO structure proved to be of crucial importance for the obtaining of highly stabilised Pt NPs (no metal leaching was detected) with small dimensions (<1.5 nm). Additionally, recycling studies showed that it was possible to use catalyst **66** up to five cycles without any significant loss of catalytic activity and selectivity. Hybrid material **67** was used as catalyst for *S*-arylation reaction involving the coupling of benzylic and aromatic thiols with aryl halides (Scheme 24). High yields of the desired products using low Pd loadings were achieved and the robustness of catalyst **67** was proved carrying out up to 10 cycles without loss of activity.

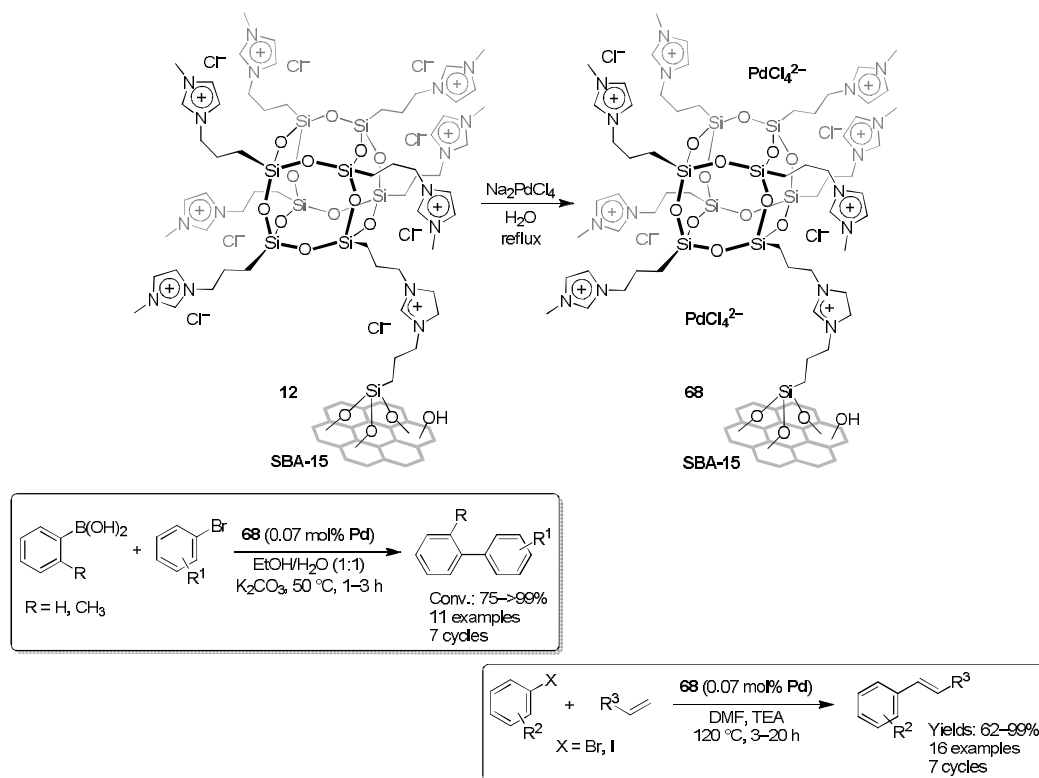


Scheme 23. Chemical functionalisation of the inner surface of fused-silica microfluidic capillaries and their use in the reduction of nitrobenzene derivatives and hydrosilylation of phenylacetylene with triethylsilane.



Scheme 24. Synthesis of Pt@IL-PMO 66 and Pd@IL-PMO 67 and their application in the aerobic oxidation of alcohols in water and *S*-arylation couplings.

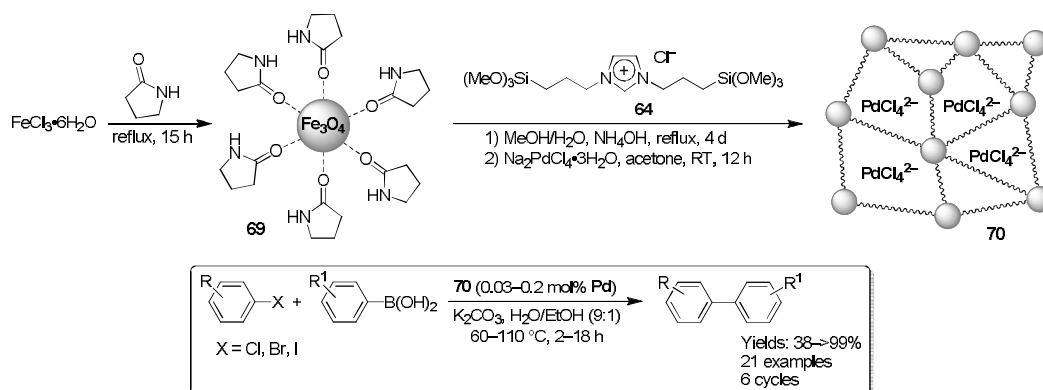
According to the procedure reported in Scheme 3, a highly porous silica SBA-15 was functionalised with POSS that was used as scaffolds for imidazolium moieties giving rise to hybrid **12**, which was decorated with Pd species by anionic metathesis reaction between chloride ions and PdCl_4^{2-} affording material **68** (Scheme 25). The hybrid **68** was used as catalyst in the Suzuki and Heck reactions.³⁰ This palladium nanocomposite showed very high catalytic activity in both Suzuki and Heck reactions using very low Pd loading down to 0.007 mol% approaching to outstanding TOF values of 114,286 and 32,381 h^{-1} , respectively. The excellent results were ascribed to the synergistic combination between the textural properties of the SBA-15 support and the presence of the imidazolium-POSS nanocage within the pores of SBA-15, enabling the production of a sort of nanoreactor with internal diffusion paths. Recycling studies in both the C–C coupling reactions revealed the good stability of catalyst **68** that was reused up to seven cycles without loss of catalytic activity. Interestingly, only Pd(II) was detected in the reused catalyst in the Heck reaction, and this finding was explained by invoking the formation of highly stabilised anionic Pd(0) species that were quickly re-oxidised by air after the completion of the reaction.



Scheme 25. Synthesis of Pd(II) imidazolium functionalised POSS hybrid **68** and its catalytic application in the Suzuki and Heck reactions.

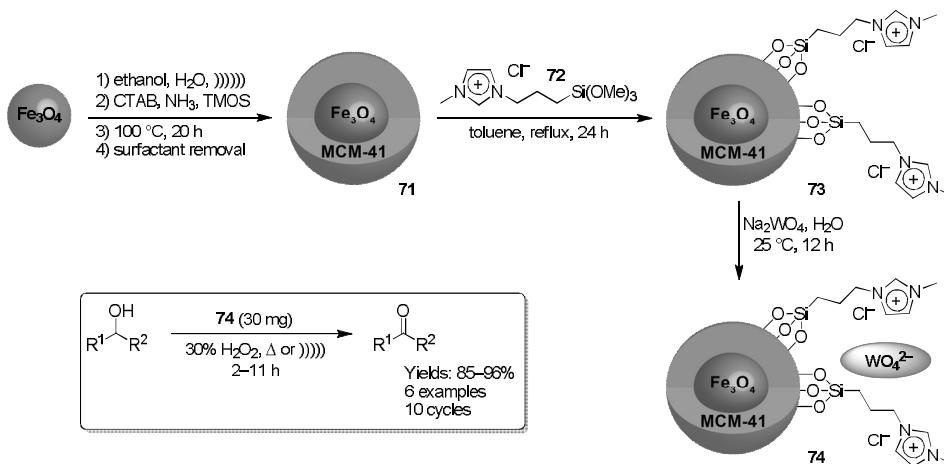
A thermal decomposition route was applied for the formation of ultrasmall iron oxide NPs obtained with the aim to achieve the formation of a novel magnetic ionic nanoparticle network (MINN) by means of the use of the dialkyl imidazolium bridge **64**. The synthetic route for the production of hybrid network system started from the preparation of water-soluble iron oxide NPs (5–7 nm) **69** by refluxing $\text{FeCl}_3 \cdot 6\text{H}_2\text{O}$ in 2-pyrrolidone. In the next stage, iron oxide NPs **69** were dispersed in a mixture of water/methanol and treated with ammonia to remove 2-pyrrolidone from the surface of NPs prior to add **64**. This allowed obtaining the magnetic ionic nanoparticle network that was used as suitable support material for PdCl_4^{2-}

through a simple ion exchange with Cl^- giving rise to Pd@MINN hybrid **70** (Scheme 26).³¹ Pd@MINN **70** was successfully applied as catalyst in the Suzuki reaction of high challenging substrates comprising aryl chlorides and heteroaryl halides. A simple recycling procedure involving a magnetic decantation was followed by means of the use of an external magnet for the recovering of the catalyst **70**. Only slight loss of catalytic activity was revealed during the six cycles explored. Furthermore, the hot filtration test as well as the use of some poisoning materials such as mercury, poly-(4-vinylpyridine), and SBA-propyl-SH showed how catalyst **70** acted as a reservoir for homogeneous active Pd species.



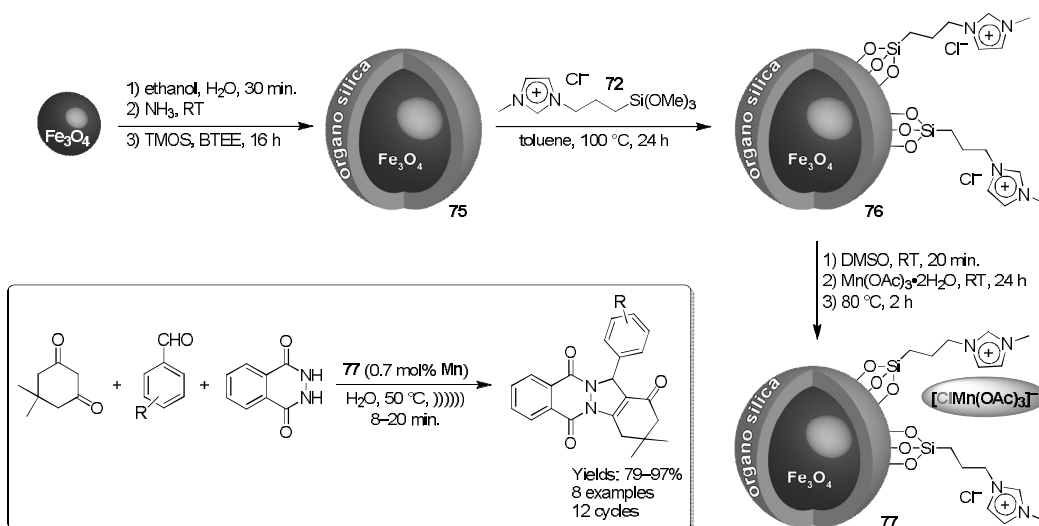
Scheme 26. Preparation of Pd@MINN **70** and its use in the Suzuki reaction.

Elhamifar *et al.* used magnetite iron oxide covered with a layer of silica MCM-41 using CTAB surfactant and TMOS as silica precursor under basic conditions giving rise to a core-shell structured material **71**. Subsequently, 1-methyl-(3-trimethoxysilylpropyl) imidazolium chloride **72** was grafted onto the surface of **71** to afford **73**, which was treated with Na_2WO_4 to produce the $\text{Fe}_3\text{O}_4\text{@MCM@IL-WO}_4^{2-}$ nanocomposite **74**. The resulting hybrid material **74** was applied as powerful catalyst for the green oxidation of alcohols in the presence of H_2O_2 both under thermal and ultrasonic conditions (Scheme 27).³² The recoverability by means of an external magnet and the reusability of this catalyst were tested over 10 cycles and only a slight decrease of the catalytic activity was reported. Moreover, leaching test confirmed that there was no leaching of active species during the reaction process.



Scheme 27. Synthesis of $\text{Fe}_3\text{O}_4\text{@MCM@IL-WO}_4^{2-}$ **74** and its use as catalyst for alcohols oxidation.

In another work, Elhamifar *et al.* covered the magnetite nanoparticles with an organosilica (OS) layer obtained by the simultaneous use of TMOS and 1,2-bis(triethoxysilyl)ethane (BTEE) precursors. The resulting material **75** was functionalised with IL **72** to afford the hybrid material **76**. The final treatment with manganese acetate gave rise to the core-shell structured $\text{Fe}_3\text{O}_4@OS/IL\text{-Mn}$ material **77**. The $\text{Fe}_3\text{O}_4@OS/IL\text{-Mn}$ **77** was applied as catalyst for the one-pot preparation of biologically useful 2H-indazolo-[2,1-b]-phthalazin-triones in aqueous medium and under ultrasonic conditions (Scheme 28).³³ The recoverability as well as the durability of nanocatalyst **77** was studied under the optimised reaction conditions. It was possible to reuse the $\text{Fe}_3\text{O}_4@OS/IL\text{-Mn}$ **77** up to twelve cycles with only a low decrease of catalytic activity during the recycling. The heterogeneous nature of the catalytic process was proved by means of a leaching experiment that confirmed the absence in solution of any catalytically active species after the catalyst removal through an external magnet.

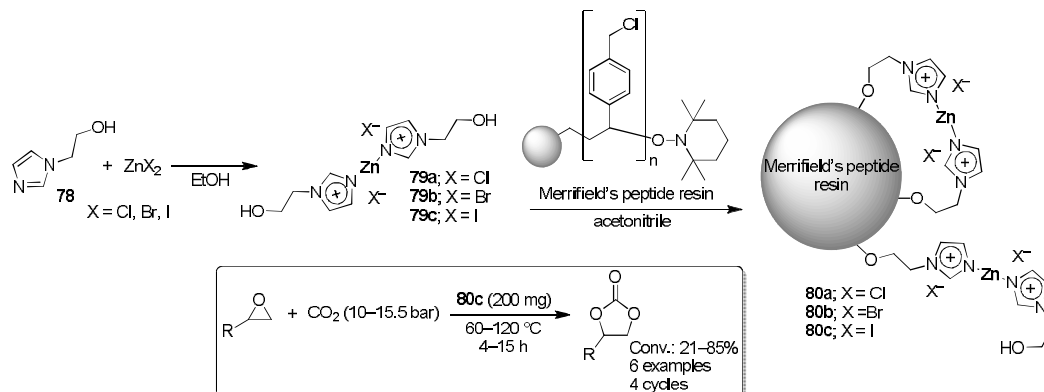


Scheme 28. Synthetic route followed for the preparation of $\text{Fe}_3\text{O}_4@OS/IL\text{-Mn}$ **77** and its application in the synthesis of 2H-indazolo-[2,1-b]-phthalazin-triones.

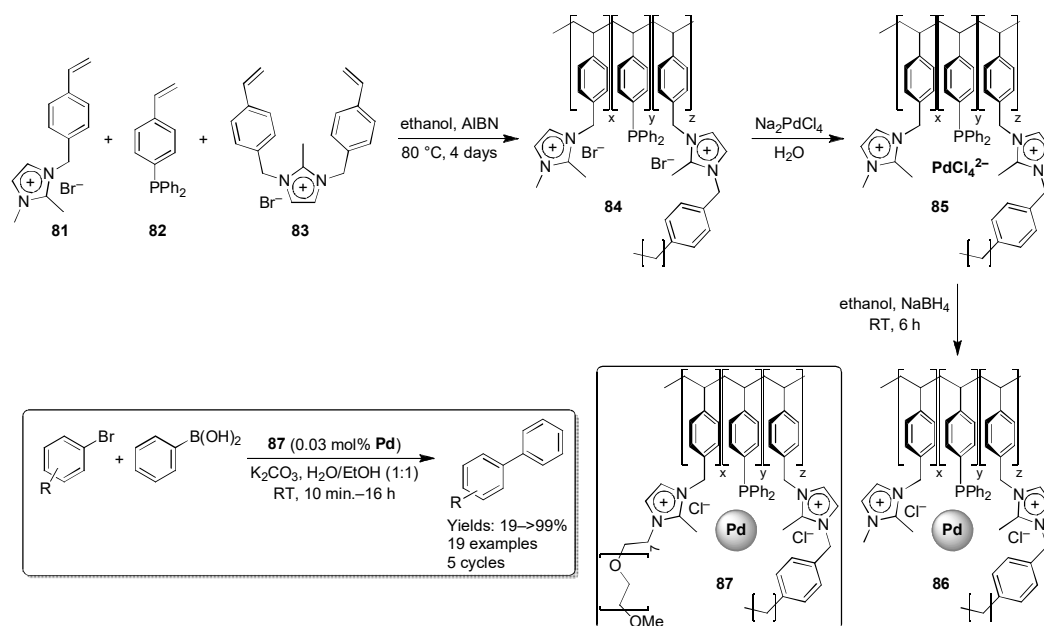
A structurally modified polystyrene-based support obtained starting from a Merrifield's peptide resin was employed to immobilise Zn-containing imidazolium salts bearing different counterions (Cl^- , Br^- , or Γ^-). The synthetic procedure involved the initial reaction between 1-(2-hydroxyethyl)imidazole **78** and different zinc halides to afford bis[1-(2-hydroxyethyl)imidazolium]zinc **79a-c** by metal insertion. The final immobilisation of **79a-c** onto Merrifield's peptide resin by alkoxylation yielded materials **80a-c** (Scheme 29).³⁴ The hybrid **80** was designed with the aim to exploit synergistic effects between the metal centre and the nucleophilic anion in order to use it as a bifunctional catalyst for the chemical fixation of CO_2 into epoxides for the synthesis of cyclic carbonates under solvent-free conditions. Catalyst **80c** revealed to be the more active in accordance with the order of the halide ion nucleophilicity: $\text{Cl}^- < \text{Br}^- < \Gamma^-$. Moreover, material **80c** was successfully used for four cycles without any leaching of active species or significant loss of catalytic activity. Both batch (closed system) and semibatch (allowing for CO_2 addition during the reaction) reactors for the synthesis of cyclic carbonates were employed. Kinetic studies and process optimisation using the response surface methodology allowed demonstrating the advantage of the semibatch system over the batch one.

Polystyrene-based polymer **84** was prepared by AIBN-initiated radical polymerisation of imidazolium-modified styrene monomer **81**, diphenylphosphine-modified styrene **82** as heteroatom donor, and imidazolium-based cross-linker **83**. Polymer **84** was impregnated with PdCl_4^{2-} by ion exchange in water to afford **85** as brown-red solid. The following treatment with NaBH_4 led to the formation of supported Pd

NPs with the obtaining of a black material **86**, which was used as highly efficient catalysts for the Suzuki-Miyaura reaction under mild conditions (Scheme 30).³⁵ Moreover, incorporation of polyethylene glycol (PEG) into system **86** to afford material **87** improved catalyst efficacy by improving dispersibility and facilitating access to the active site. It was demonstrated that *in situ* prepared catalysts (formed by the reduction of the immobilised PdCl_4^{2-} ions to Pd^0 using phenylboronic acid) showed comparable or higher catalytic activity than the *ex situ* prepared catalysts (reduction by means of NaBH_4) **86** and **87**. The influence of diphenylphosphine donor, IL moiety, and PEG on the catalytic performance was studied and clearly showed how each component had a direct effect on the final activity of the catalyst. The recyclability of catalyst **87** in the Suzuki reaction between 4-bromoacetophenone and phenylboronic acid was tested for five consecutive runs. Only a slight decrease in catalytic activity was observed.

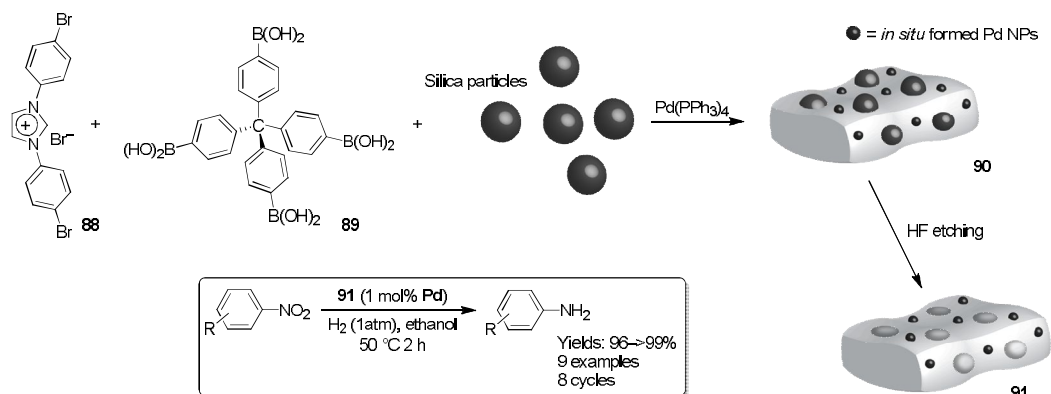


Scheme 29. Preparation of the polystyrene resin supported Zn-IL **80** and its catalytic application in the synthesis of cyclic carbonates from CO₂ and epoxides.



Scheme 30. Preparation of the polystyrene supported Pd-PPh₂-IL **86** and Pd-PPh₂-IL-PEG **87** and catalytic application in the Suzuki reaction.

Wang *et al.* synthesised a series of imidazolium-based porous organic polymers (Im-POP) containing palladium NPs. Pd NPs, which due to the strong interaction with the imidazolium moieties showed a narrow size distribution, were formed *in situ* by the decomposition of tetrakis(triphenylphosphine)palladium(0). The latter was used as catalyst for the preparation of the polymer **90** obtained by means of the Suzuki coupling between 1,3-bis(4-bromophenyl)imidazolium bromide **88** and (methane-tetra-4,1-phenylene)tetrakisboronic acid **89** in the presence of different amount of SiO₂ particles. The following etching of **90** with HF afforded the ionic porous organic polymer Pd@-Im-POP **91** (Scheme 31).³⁶ The appropriate use of an optimal amount of SiO₂ template resulted in a marked enhancement of the catalytic activity of the polymeric network **91** in the hydrogenation of nitroarenes using H₂ as reductive agent owing to the best pore properties (meso- and macropores) of the catalyst **91** that facilitate the mass transfer of substrates during the reaction. Reusability of catalyst **91** was tested for eight consecutive runs in the hydrogenation of 1-*tert*-butyl-4-nitrobenzene using NaBH₄ as the reductant. Only a slight decrease in the catalytic activity was revealed, whereas no leaching of Pd species or clear aggregation of Pd NPs was observed.

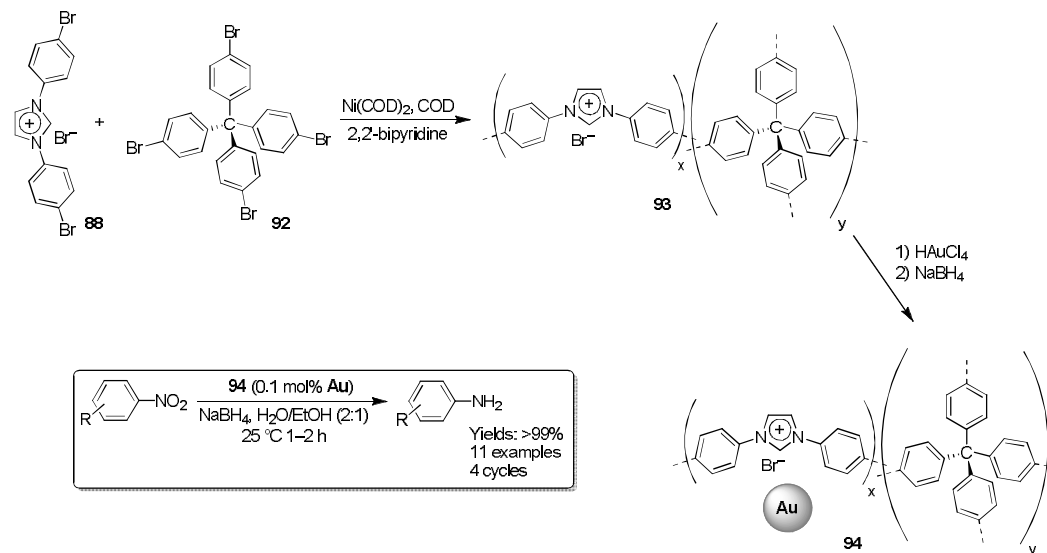


Scheme 31. Preparation of Pd@-Im-POP **91** and its application in the hydrogenation of nitroarenes.

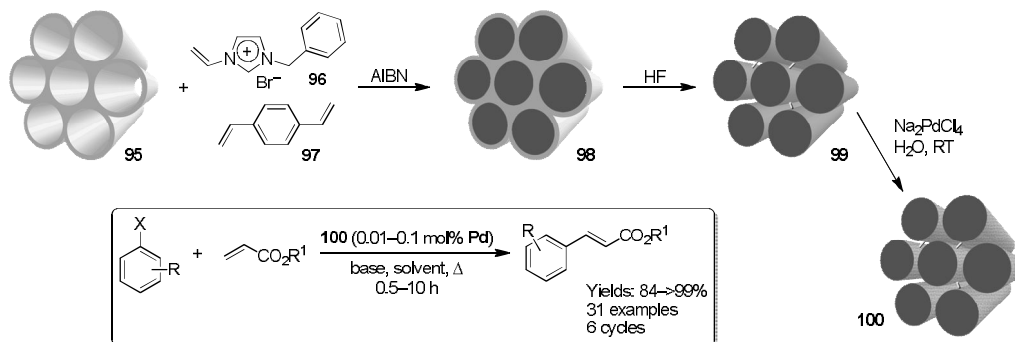
In another work, Wang *et al.*, developed another method to gain access to ionic polymers that were not affected by metal contamination arising from the synthetic procedure. With this in mind, the nickel-catalysed Yamamoto reaction was chosen as an alternative synthetic tool for ionic polymers due to the ease removal of the nickel species by treatment with inorganic acid during the work up procedure. This alternative path allowed for the use of imidazolium-based polymers as support for different metal species such as gold. The synthesis of the polymeric network **93** was achieved by the Yamamoto reaction between 1,3-bis(4-bromophenyl)imidazolium bromide **88** and tetrakis(4-bromophenyl)methane **92** catalysed by bis(1,5-cyclooctadiene)nickel(0) (Ni(COD)₂). Subsequently, polymer **93** was treated with aqueous HAuCl₄ and reduced with NaBH₄ to generate Au@Im-POP **94** that was tested in the reduction of nitroarenes using NaBH₄ as reducing agent (Scheme 32).³⁷ The positive influence of both the imidazolium moieties and the surface area of Au@Im-POP **94** on the catalytic activity was demonstrated by comparison with the non-ionic polymer arising from the Yamamoto reaction of **92**, which showed a decreased catalytic activity. Moreover, recyclability studies proved how catalyst **94** was more stable (4 runs) and showed only slight agglomeration of Au NPs compared to the non-ionic analogue that lost most of its catalytic activity and suffered from Au NPs agglomeration after the second run.

An ordered mesoporous cross-linked polymer with IL moieties was prepared and used as support for highly dispersed Pd NPs with a narrow size distribution (2-4 nm). *O*-silylated SBA-15 **95** was chosen as hard template because of its highly ordered structure and 3D microporous connectivity. Silylation of the surface hydroxyl groups of the pristine SBA-15 was carried out with the aim of increase its hydrophobicity to facilitate the diffusion of the hydrophobic reactants inside the pores. The preparation of the polymeric material **97** started with the charging of the channel of silylated SBA-15 with a mixture of

3-benzyl-1-vinyl-1*H*-imidazolium bromide **96**, divinylbenzene (DVB) **97** and AIBN as radical initiator to afford material **98**. The removal of the SBA-15 template with a HF solution gave rise to the ordered mesoporous polymer (OMP-IL-Bn) **99** that was used as support for Pd NPs formed after the exchange of bromide with tetrachloropalladate ions with the formation of material Pd@OMP-IL-Bn **100** (Scheme 33).³⁸ Notably, despite of the absence of any reducing agent, Pd NPs were probably formed because of traces of reducing solvents inside the polymer backbone. Pd@OMP-IL-Bn **100** showed high catalytic activity in the Heck reaction between aryl halides and different acrylates using low catalytic loadings (0.01-0.1 mol% Pd) with the adoption of optimised reaction conditions and the use of specific additives when highly challenging aryl chlorides were reacted. Reusability tests of the catalyst showed that Pd@OMP-IL-Bn **100** preserved its catalytic activity in six consecutive Heck couplings. TEM analysis revealed an increased mean diameter of the supported Pd NPs (5-11 nm) that were still highly dispersed over the polymer support.



Scheme 32. Preparation of Au@-Im-POP **94** and its application in the hydrogenation of nitroarenes.

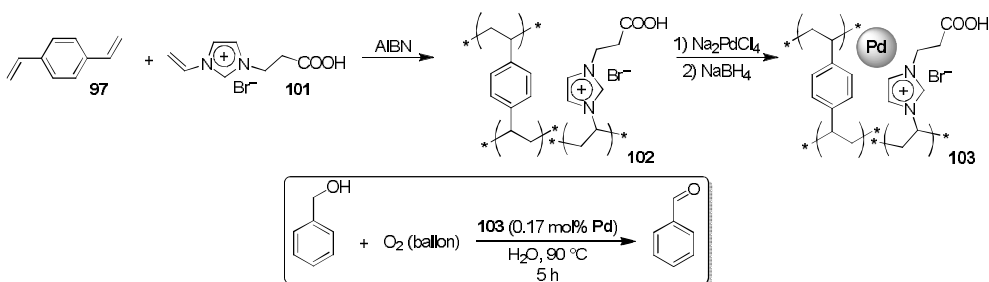


Scheme 33. Preparation of Pd@OMP-IL-Bn **100** and its use as catalyst in the Heck reaction between aryl halides and different acrylates.

Both hot filtration and Hg^0 poisoning test furnished evidences about the homogeneous nature of the catalytic process. Pd@OMP-IL-Bn **100** acted as a sort of reservoir for soluble active Pd species that were

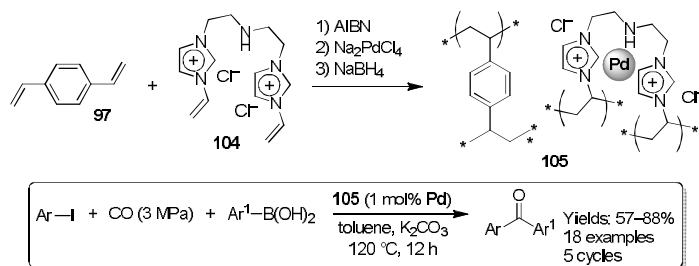
redeposited over the polymeric support because of the presence of the IL moieties that were able to efficiently recapture them from the reaction mixture at the end of the catalytic process.

A series of cross-linked mesoporous poly(ionic liquids) (MPILs) were obtained by means of the free radical copolymerization of DVB **97** and imidazolium salts-based ILs functionalised with different groups. These MPILs were used as support for Pd NPs generated after the ion exchanging with Na_2PdCl_4 and the subsequent reduction with NaBH_4 . For this purpose, the choice of the IL tethered with a carboxylic group IL-COOH **101** along with the use of the proper ratio between **97** and **101** was found to be crucial to impart key features to the copolymeric skeleton **102** (such as high ionic density and large surface area), fundamental for obtaining of highly uniform and narrow size dispersed Pd NPs obtained in the material Pd@PIL-COOH **103** (Scheme 34).³⁹ The presence of both hydrophilic (IL-COOH) and hydrophobic (DVB) monomers were accountable for the special amphiphilicity of the resultant copolymer that allowed Pd@PIL-COOH **103** to be used as catalyst in the selective oxidation of benzyl alcohol to the corresponding aldehyde with O_2 in aqueous medium. The crucial role played by the imidazolium moiety in the copolymer **103** was proved by the comparison of its catalytic activity with that of the polymer arising from the polymerization of DVB onto which Pd NPs were supported. The homopolymer showed a lower activity due to the lack of the ionic sites able to stabilise the charged Pd NPs precursors (PdCl_4^{2-} ions) giving rise to small and well dispersed metal nanoparticles. Recyclability of catalyst **103** was studied carrying out five consecutive cycles without any loss of catalytic activity, metal leaching or Pd NPs agglomeration.



Scheme 34. Synthesis of Pd@PIL-COOH **103** and its catalytic application in the oxidation of benzyl alcohol to benzaldehyde with O_2 in water.

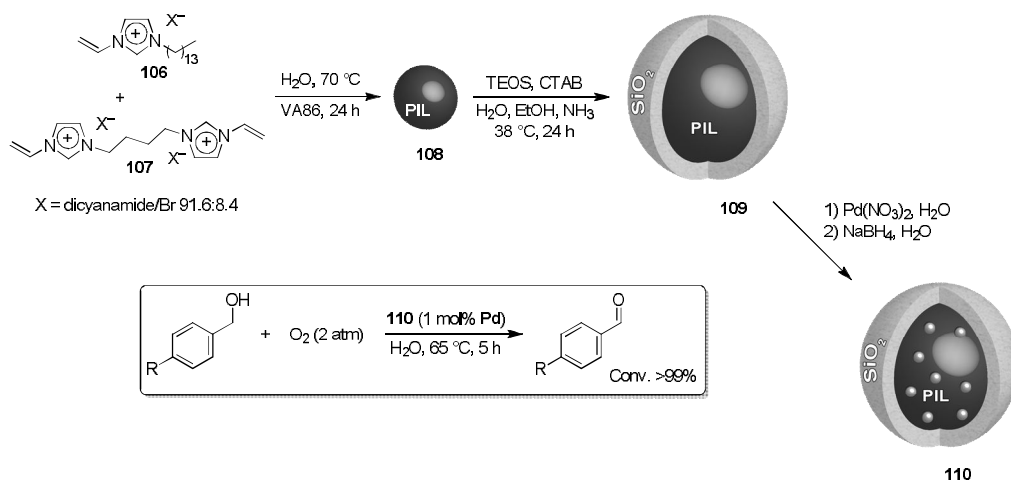
Liu *et al.* reported another example regarding the preparation of cross-linked polymeric materials based on poly(ionic liquids) in which the AIBN-initiated copolymerization of a dication imidazolium ionic liquid modified with an amine group **104** with DVB **97** followed by the palladium immobilisation by ion exchange with PdCl_4^{2-} and the subsequent reduction with NaBH_4 afforded material **105** (Scheme 35).⁴⁰ The use of a 1:1 mole ratio between **97** and **104** afforded a copolymer able to efficiently stabilise Pd NPs that were well dispersed over the surface of material **105** used as catalyst for the carbonylative Suzuki coupling reaction of aryl iodides with aryl boronic acids to give the corresponding products. Hot filtration and Hg^0 poisoning tests afforded evidences that the leached palladium species during the course of the reaction were recaptured onto the polymer after the reaction was completed.



Scheme 35. Synthesis of material **105** and its application in the carbonylative Suzuki coupling reaction.

Catalyst **105** was tested in five consecutive cycles with a small decrease of its catalytic activity attributed to leaching of Pd and slight aggregation of Pd NPs.

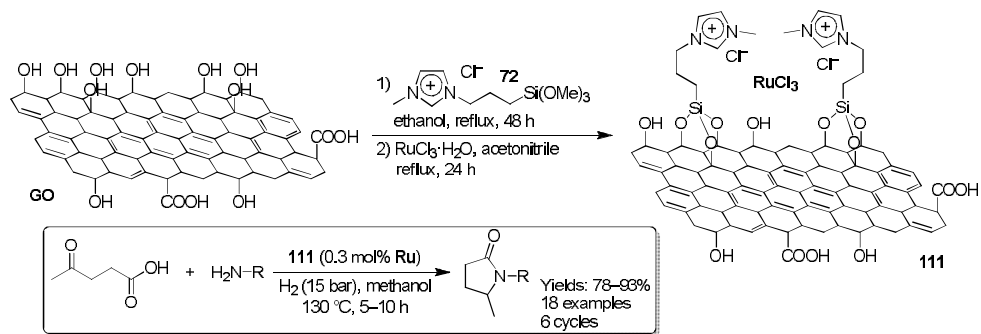
A hybrid micelle-like nanoreactor formed by a PILs core and a mesoporous silica shell was developed and used as support for Pd NPs. The preparation of the nanoreactor **110** started with the dispersion polymerization of 3-tetradecyl-1-vinyl-imidazolium ionic liquid monomer **106** with the bis-vinylimidazolium salt **107** as cross-linker in the presence of the water-soluble non-ionic azo initiator VA86 to afford the PIL nanospheres **108**. The following coating with a thin layer of mesoporous silica using TEOS as silica source was carried out by means of the assistance of surfactant CTAB to produce the core-shell structure **109**. The inorganic shell acts as an “exoskeleton” providing high mechanical/chemical stability and hydrophilic behaviour to the nanoreactor, whereas the residual CTAB aggregates inside the mesopores play a double role preventing the diffusion of PIL chains out of the silica shell and promoting the transition of hydrophobic molecules from water to the PIL core. Material **109** was subjected to the anion exchange with Pd(NO₃)₂ followed by reduction with NaBH₄ to generate the nanoreactor **110**, which was characterised by the presence of highly dispersed Pd NPs (~2 nm) mainly located around the PIL core. The nanoreactor **110** was tested as catalyst for the selective oxidation of benzyl- and 4-methoxy-benzyl alcohols to the corresponding aldehydes in water (Scheme 36).⁴¹ To prove the advantages of the design of nanoreactor **110**, its catalytic performances was compared with two additional catalysts, namely MCM-41-Pd and PIL-Pd. In both cases, catalyst **110** showed higher catalytic activity toward both substrates, however, during the recycling tests a slightly decrease in the desired product yield after the fourth cycle was observed.



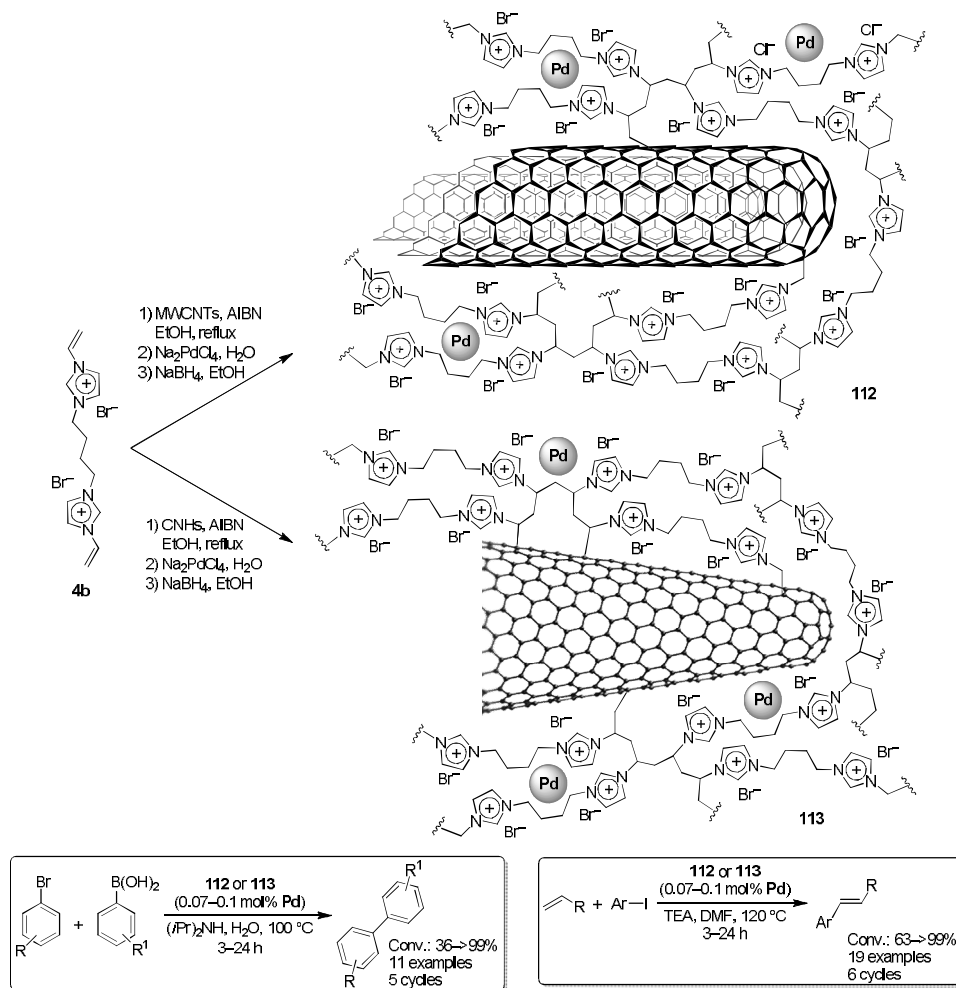
Scheme 36. Synthesis of nanoreactor **110** and its catalytic performance in the oxidation of benzyl alcohols.

Graphene oxide (GO) was modified through grafting of 1-methyl-(3-trimethoxysilyl)propyl imidazolium chloride **72** on its surface followed by the reaction with RuCl₃·3H₂O to afford Ru@GO-IL **111**, which was tested as catalyst for the reductive amination of biomass derived levulinic acid for the synthesis of *N*-substituted pyrrolidones in excellent yields (Scheme 37).⁴² Catalyst reusability was tested for six consecutive runs and a progressive loss of catalytic activity was detected. Further investigations proved that no metal leaching occurred, however TEM analysis of the recycled catalyst showed the formation of Ru NPs in the range of <20 nm.

The direct polymerisation of the bis-vinylimidazolium salt **4b** onto two different carbon nanoforms, namely MWCNTs and carbon nanohorns (CNHs), led to the formation of a polymeric network, which formed a cylindrical or spherical coating for MWCNTs and CNHs, respectively, as witnessed by TEM images. The ion exchange between bromide and PdCl₄²⁻ ions and the following reduction with NaBH₄ produced materials MWCNT-imi-Pd **112** and CNH-imi-Pd **113** (Scheme 38).⁴³



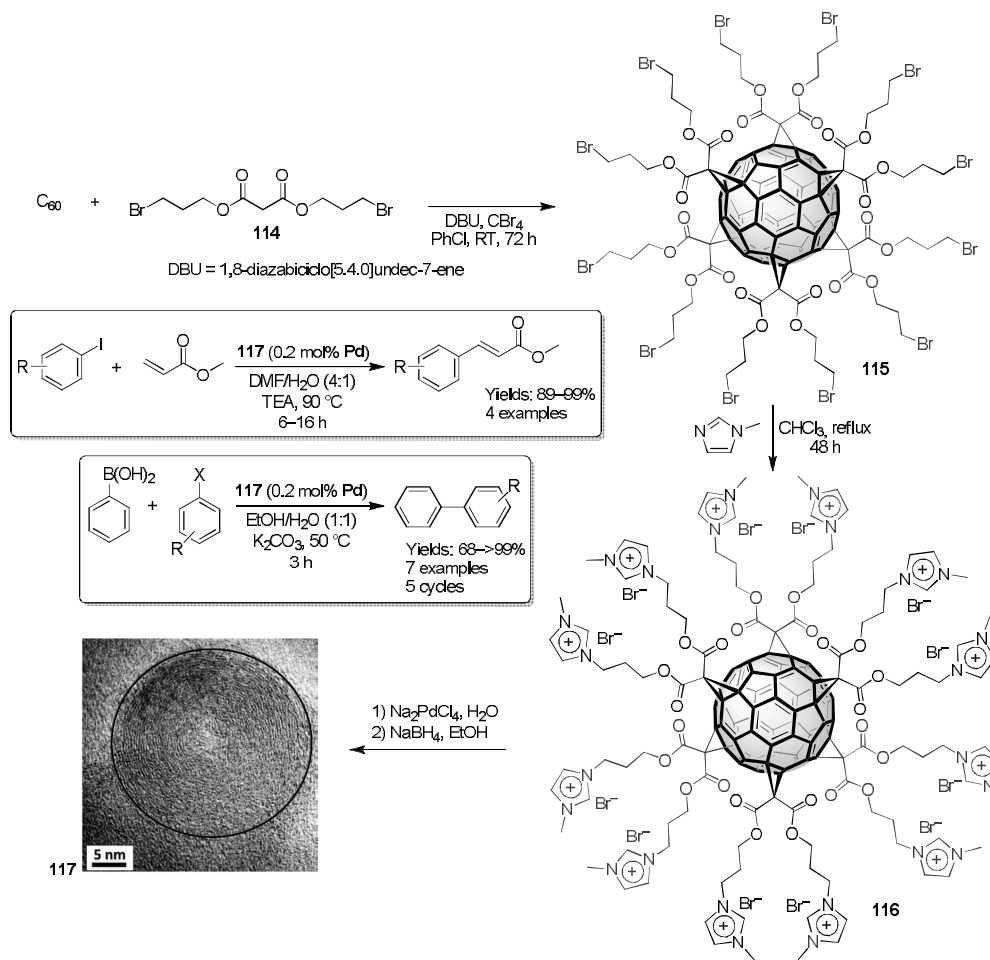
Scheme 37. Synthesis of Ru@GO-IL **111** and its application in the reductive amination of levulinic acid for the synthesis of *N*-substituted pyrrolidones.



Scheme 38. Preparation of MWCNT-imi-Pd **112** and CNH-imi-Pd **113** and their application in the Suzuki and Heck reactions.

TEM analysis showed how materials **112** and **113** had a different distribution of the formed Pd NPs on their surfaces. Indeed, MWCNT-imi-Pd **112** showed a fine dispersion of Pd NP on its whole surface, whereas Pd NPs in CNH-imi-Pd **113** were bigger and mainly located on the external surface of such material. Both MWCNT-imi-Pd **112** and CNH-imi-Pd **113** were tested as catalysts in the Suzuki and Heck reactions. Suzuki reactions were carried out in aqueous medium under aerobic conditions. CNH-imi-Pd **113** showed to be slightly more active than material **112** and this behaviour was ascribed to the higher superficial exposure of Pd NPs in the CNH-based material. Moreover, both catalysts showed excellent activity and recyclability in the investigated C–C coupling reactions without loss of catalytic activity.

Fullerene C_{60} was used as molecular scaffold for the preparation of a series of new C_{60} -IL hybrids in which both the number of IL moieties (two or twelve) and the nature of anion and cation was varied. One of these hybrids, namely hexakis adduct **116**, was chosen as support for Pd NPs.⁴⁴ The synthetic route, reported in Scheme 39, started with the reaction between the malonate **114** and fullerene C_{60} to afford the highly symmetric hexakis adduct **115**, which after the reaction with 1-methylimidazole generated hexa-IL- C_{60} **116**. Due to the high functionalisation degree of this hexakis adduct that results in a high local concentration of imidazolium moieties (twelve units), hexa-IL- C_{60} **116** was chosen as an optimal support for the grown of Pd NPs.



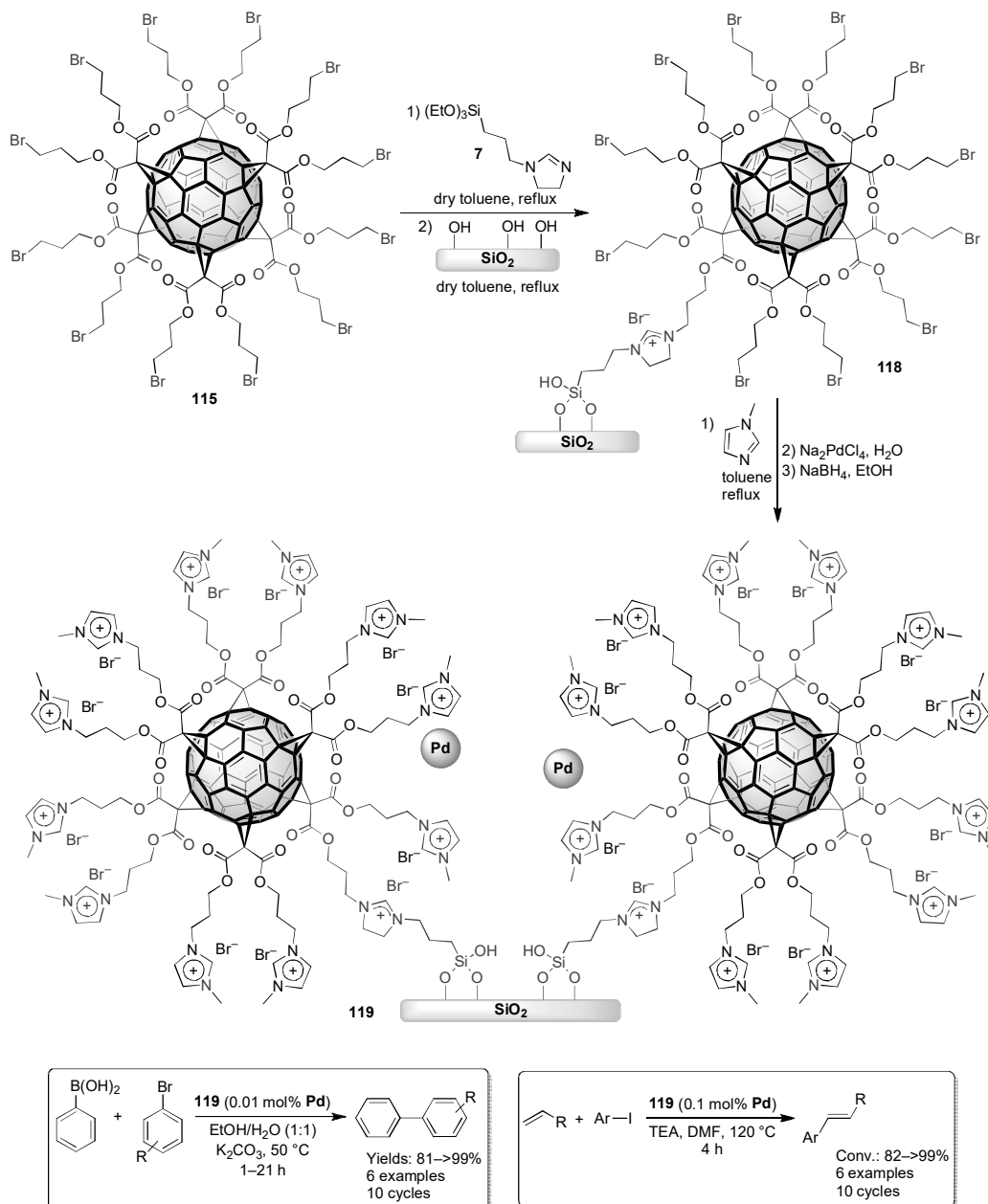
Scheme 39. Preparation of material **117** and its application in the Suzuki and Heck reactions.

Surprisingly, the reduction with NaBH_4 of the previously immobilised Pd(II) species gave rise to an insoluble and finely dispersed black powder **117**. TEM analysis revealed that **117** was formed by large graphitic domains and organised nanostructures such as several carbon nano-onions with diameters in the 20-30 nm range along with uniformly distributed Pd NPs of a mean diameter of 1.4 nm. Material **117** was used as catalyst in the Suzuki and Heck reactions with a loading of 0.2 mol% with good results. Moreover, recyclability of material **117** was tested in the Suzuki reaction between 4-bromobenzaldehyde and phenylboronic acid for five cycles and no loss of catalytic activity was detected.

With the aim to optimize the IL-phase distribution onto the surface of different support materials that should guarantee an enhanced stabilisation of the *in situ* formed Pd NPs, and encouraged by the good results obtained with catalytic material **117**, a new synthetic strategy for the immobilisation of C_{60} -IL derivatives onto inert supports was designed (Scheme 40). Amorphous silica proved to be the best choice for the obtaining of the durable and easily recoverable catalytic material **119**. The synthesis of the hybrid material **119** started with the reaction between triethoxy-3-(2-imidazolin-1-yl)propylsilane **7** and the C_{60} derivative **115** followed by the grafting of the obtained intermediate onto the silica support to afford material **118**. The subsequent reaction of **118** with 1-methylimidazole followed by the immobilisation of PdCl_4^{2-} ions and the final reduction with NaBH_4 allowed to obtain SiO_2 - C_{60} -IL-Pd **119** (Scheme 40).⁴⁵ Material **119** was tested as catalyst in the Suzuki and Heck reactions. Noteworthy, the corresponding material supported onto SBA-15 was able to catalyse the Suzuki reaction between phenylboronic acid and 4-bromoacetophenone in $\text{H}_2\text{O}/\text{EtOH}$ using K_2CO_3 as base at 120 °C with a very low loading of 0.0005 mol%, reaching TON and TOF values of 182,000 and 3,640,000 h^{-1} , respectively. Catalyst **119** showed its longevity in the recycling tests. Indeed, it was possible to carry out up to ten cycles both in the Suzuki and Heck reactions with only a slight decrease of the catalytic activity in the tenth cycle of the latter process. In both catalytic processes, after the removal of the catalyst from the reaction mixture, no palladium leaching was detected (Scheme 40).

Halloysite nanotubes (HNTs) have been used as supports for the production of imidazolium-based hybrid materials. HNTs are composed by double-layered aluminosilicate minerals that has a predominantly hollow tubular structure. Halloysite nanotubes were functionalised through the grafting of 3-mercaptopropyl trimethoxysilane on the external surface of HNTs by microwave (MW) irradiation to afford material **120** that was reacted with 3-octyl-1-vinyl-imidazolium bromide **121** by a thiol-ene reaction. MW irradiation allowed to achieve a higher functionalisation degree of the HNT surface compared with that obtained through conventional synthesis. The subsequent treatment with Na_2PdCl_4 in water followed by reduction with NaBH_4 gave rise to the HNT-IL-Pd **122** (Scheme 41).⁴⁶ Material **122** was tested as catalyst in the Suzuki reaction between phenylboronic acid and several aryl halides in ethanol/water with different catalytic loadings of (0.1-1.0 mol%). Reactions were carried out under microwave irradiation at 120 °C for 10 min to give the corresponding biphenyls in good to excellent yields. Up to five cycles were performed by using catalyst **122** with the higher catalytic loading.

Material **120** and the bis-vinylimidazolium salt **123** were reacted under MW irradiation in the presence of AIBN and in solvent-free conditions to afford a highly cross-linked hybrid material that was used as support for Pd NPs. The ion exchange reaction with PdCl_4^{2-} followed by the treatment with NaBH_4 gave rise to material **124** (Scheme 42).⁴⁷ TEM analysis of the resulting material **124** showed that Pd NPs (9.4±3.7 nm) were uniformly dispersed on the surface of the polymeric network, which covered all the surface of HNTs. Once again, Suzuki and Heck reactions were chosen to assess the catalytic activity of material **124**. The optimised reaction conditions under MW irradiation allowed to obtain good results in both processes. Recyclability of **124** was also evaluated carrying out up to ten consecutive cycles for the Suzuki reaction without any change in its catalytic activity, whereas, in the ninth cycle of the Heck reaction, a small drop of the activity of **124** was reported. Further experiments proved that **124** mainly acted as a reservoir of soluble Pd species that were redeposited onto the support material at the end of the reaction. Moreover, TEM analysis showed that there was a slight agglomeration of Pd NPs, whereas, in the case of the Heck reaction, a Pd leaching corresponding to 20 wt% of the total amount of immobilised Pd at the end of the investigated nine cycles was detected.

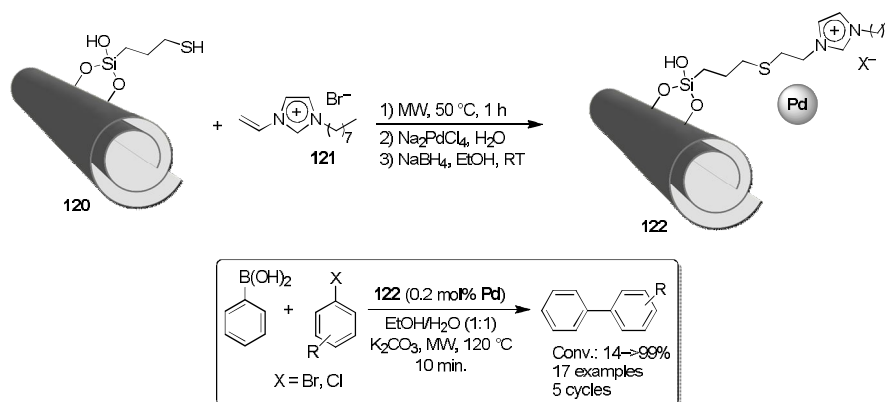


Scheme 40. Preparation of material **119** and its application in the Suzuki and Heck reactions.

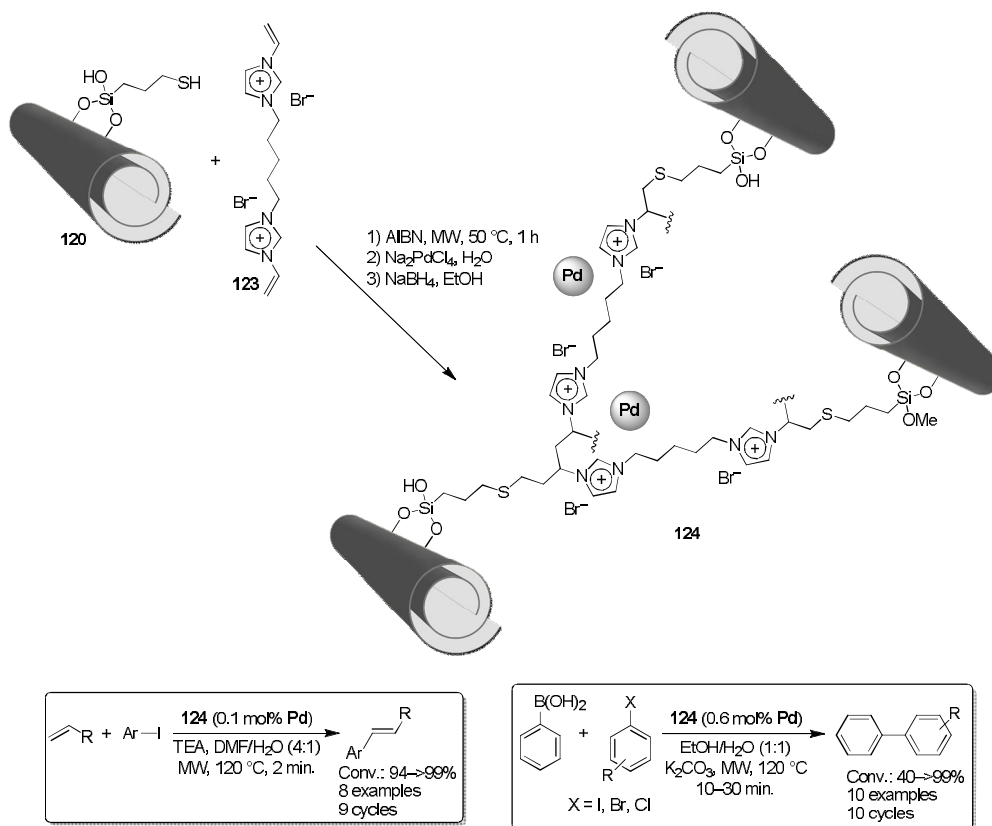
4. Conclusions

In conclusion, we have here reported the wide applications of covalently supported imidazolium salts as very useful catalytic materials in many synthetic transformations. The usefulness of these systems can be observed both in the metal-free based reactions, such as cycloaddition of CO_2 to epoxides, Michael addition, transesterification, Knoevenagel reactions and selected metal-catalysed reactions such as Suzuki and Heck

coupling reactions, hydrogenation, oxidation of alcohols, hydrosilylation of alkynes, *etc.* The role of the proper support in enhancing catalytic properties and easy recovery and reuse of such materials has been highlighted.



Scheme 41. Preparation of HNT-IL-Pd **122** and its catalytic application in the Suzuki reaction.



Scheme 42. Preparation of material **124** and its catalytic application in the Suzuki and Heck reactions.

Acknowledgements

This work was financially supported by the University of Palermo.

References

- Han, L.; Choi, H.-J.; Choi, S.-J.; Liu, B.; B. Park, B. *Green Chem.* **2011**, *13*, 1023-1028.
- Liu, M.; Lu, X.; Jiang, Y.; Sun, J.; Arai, M. *ChemCatChem* **2018**, *10*, 1860-1868.
- Aprile, C.; Giacalone, F.; Agrigento, P.; Liotta, L. F.; Martens, J. A.; Pescarmona, P. P.; Gruttadauria, M. *ChemSusChem* **2011**, *4*, 1830-1837.
- Agrigento, P.; Al-Amsyar, S. M.; Sorée, B.; Taherimehr, M.; Gruttadauria, M.; Aprile, C.; Pescarmona, P. P. *Catal. Sci. Technol.* **2014**, *4*, 1598-1607.
- Calabrese, C.; Liotta, L. F.; Giacalone, F.; Gruttadauria, M.; Aprile, C. *ChemCatChem* **2019**, *11*, 560-567.
- Calabrese, C.; Fusaro, L.; Liotta, L. F.; Giacalone, F.; Comès, A.; Campisciano, V.; Aprile, C.; Gruttadauria, M. *ChemPlusChem* **2019**, *84*, 1536-1543.
- Lee, J. H.; Lee, A. S.; Lee, J.-C.; Hong, S. M.; Hwang, S. S.; Koo, C. M. *ACS Appl. Mater. Interfaces* **2017**, *9*, 3616-3623.
- Han, L.; Li, H.; Choi, S.-J.; Park, M.-S.; Lee, S.-M.; Kim, Y.-J.; Park, D.-W. *Appl. Catal., A* **2012**, *429-430*, 67-72.
- Buaki-Sogó, M.; Vivian, A.; Bivona, L. A.; García, H.; Gruttadauria, M.; Aprile, C. *Catal. Sci. Technol.* **2016**, *6*, 8418-8427.
- Calabrese, C.; Liotta, L. F.; Carbonell, E.; Giacalone, F.; Gruttadauria, M.; Aprile, C. *ChemSusChem* **2017**, *10*, 1202-1209.
- Xu, J.; Xu, M.; Wu, J.; Wu, H.; Zhang, W.-H.; Li, Y.-X. *RSC Adv.* **2015**, *5*, 72361-72368.
- Zhang, W.-H.; He, P.-P.; Wu, S.; Xu, J.; Li, Y.; Zhang, G.; Wei, X.-Y. *Appl. Catal., A* **2016**, *509*, 111-117.
- Gupta, R.; Yadav, M.; Gaur, R.; Arora, G.; Sharma, R. K. *Green Chem.* **2017**, *19*, 3801-3812.
- Xu, X.; Cheng, T.; Liu, X.; Xu, J.; Jin, R.; Liu, G. *ACS Catal.* **2014**, *4*, 2137-2142.
- Ying, A.; Liu, S.; Li, Z.; Chen, G.; Yang, J.; Yan, H.; Xu, S. *Adv. Synth. Catal.* **2016**, *358*, 2116-2125.
- Wan, H.; Wu, Z.; Chen, W.; Guan, G.; Cai, Y.; Chen, C.; Li, Z.; Liu, X. *J. Mol. Catal. A: Chem.* **2015**, *398*, 127-132.
- Xie, W.; Wang, H. *Renewable Energy* **2020**, *145*, 1709-1719.
- Liu, H.; Chen, J.; Chen, L.; Xu, Y.; Guo, X.; Fang, D. *ACS Sustainable Chem. Eng.* **2016**, *4*, 3140-3150.
- Moosavi-Zare, A. R.; Zolfigol, M. A.; Zarei, M.; Zare, A.; Khakyzadeh, V. *J. Mol. Liq.* **2015**, *211*, 373-380.
- Parvin, M. N.; Jin, H.; Ansari, M. B.; Oh, S.-M.; Park, S.-E. *Appl. Catal., A* **2012**, *413-414*, 205-212.
- Luska, K. L.; Julis, J.; Stavitski, E.; Zakharov, D. N.; Adams, A.; Leitner, W. *Chem. Sci.* **2014**, *5*, 4895-4905.
- El Sayed, S.; Bordet, A.; Weidenthaler, C.; Hetaba, W.; Luska, K. L.; Leitner, W. *ACS Catal.* **2020**, *10*, 2124-2130.
- Luza, L.; Gual, A.; Rambor, C. P.; Eberhardt, D.; Teixeira, S. R.; Bernardi, F.; Baptista, D. L.; Dupont, J. *PCCP* **2014**, *16*, 18088-18091.
- Vucetic, N.; Virtanen, P.; Nuri, A.; Mattsson, I.; Aho, A.; Mikkola, J.-P.; Salmi, T. *J. Catal.* **2019**, *371*, 35-46.
- Pavia, C.; Ballerini, E.; Bivona, L. A.; Giacalone, F.; Aprile, C.; Vaccaro, L.; Gruttadauria, M. *Adv. Synth. Catal.* **2013**, *355*, 2007-2018.
- Pavia, C.; Giacalone, F.; Bivona, L. A.; Salvo, A. M. P.; Petrucci, C.; Strappaveccia, G.; Vaccaro, L.; Aprile, C.; Gruttadauria, M. *J. Mol. Catal. A: Chem.* **2014**, *387*, 57-62.
- Petrucci, C.; Strappaveccia, G.; Giacalone, F.; Gruttadauria, M.; Pizzo, F.; Vaccaro, L. *ACS Sustainable Chem. Eng.* **2014**, *2*, 2813-2819.
- Fang, H.; Chen, J.; Xiao, Y.; Zhang, J. *Appl. Catal., A* **2019**, *585*, 117186. Fang, H.; Sun, S.; Liao, P.; Hu, Y.; Zhang, J. *J. Mater. Chem. A* **2018**, *6*, 2115-2121.

29. Rostamnia, S.; Doustkhah, E.; Bulgar, R.; Zeynizadeh, B. *Microporous Mesoporous Mater.* **2016**, *225*, 272-279. Karimi, B.; Naderi, Z.; Khorasani, M.; Mirzaei, H. M.; Vali, H. *ChemCatChem* **2016**, *8*, 906-910.
30. Calabrese, C.; Campisciano, V.; Siragusa, F.; Liotta, L. F.; Aprile, C.; Gruttadauria, M.; Giacalone, F. *Adv. Synth. Catal.* **2019**, *361*, 3758-3767.
31. Karimi, B.; Tavakolian, M.; Mansouri, F.; Vali, H. *ACS Sustainable Chem. Eng.* **2019**, *7*, 3811-3823.
32. Norouzi, M.; Elhamifar, D. *Composites, Part B* **2019**, *176*, 107308.
33. Neysi, M.; Elhamifar, D.; Norouzi, M. *Mater. Chem. Phys.* **2020**, *243*, 122589.
34. Kim, D.; Ji, H.; Hur, M. Y.; Lee, W.; T. Kim, T. S.; Cho, D.-H. *ACS Sustainable Chem. Eng.* **2018**, *6*, 14743-14750.
35. Doherty, S.; Knight, J. G.; Backhouse, T.; Abood, E.; Al-shaikh, H.; Clemmet, A. R.; Ellison, J. R.; Bourne, R. A.; Chamberlain, T. W.; Stones, R.; Warren, N. J.; Fairlamb, I. J. S.; Lovelock, K. R. J. *Adv. Synth. Catal.* **2018**, *360*, 3716-3731.
36. Wang, Y.; Zhong, H.; Li, L.; Wang, R. *ChemCatChem* **2016**, *8*, 2234-2240.
37. Su, Y.; Li, X.; Wang, Y.; Zhong, H.; Wang, R. *Dalton Trans.* **2016**, *45*, 16896-16903.
38. Karimi, B.; Marefat, M. R.; Hasannia, M.; Akhavan, P. F.; Mansouri, F.; Artelli, Z.; Mohammadi, F.; Vali, H. *ChemCatChem* **2016**, *8*, 2508-2515.
39. Wang, Q.; Cai, X.; Liu, Y.; Xie, J.; Zhou, Y.; Wang, J. *Appl. Catal., B* **2016**, *189*, 242-251.
40. Jiao, N.; Li, Z.; Wang, Y.; Liu, J.; Xia, C. *RSC Adv.* **2015**, *5*, 26913-26922.
41. Yang, Y.; Ambrogi, M.; Kirmse, H.; Men, Y.; Antonietti, M.; Yuan, J. *Chem. Mater.* **2015**, *27*, 127-132.
42. Raut, A. B.; Shende, V. S.; Sasaki, T.; Bhanage, B. M. *J. Catal.* **2020**, *383*, 206-214.
43. Campisciano, V.; Calabrese, C.; Liotta, L. F.; La Parola, V.; Spinella, A.; Aprile, C.; Gruttadauria, M.; Giacalone, F. *Appl. Organomet. Chem.* **2019**, *33*, e4848.
44. Campisciano, V.; La Parola, V.; Liotta, L. F.; Giacalone, F.; Gruttadauria, M. *Chem.-Eur. J.* **2015**, *21*, 3327-3334.
45. Giacalone, F.; Campisciano, V.; Calabrese, C.; La Parola, V.; Liotta, L. F.; Aprile, C.; M. Gruttadauria, *J. Mater. Chem. A* **2016**, *4*, 17193-17206.
46. Massaro, M.; Riela, S.; Lazzara, G.; Gruttadauria, M.; Milioto, S.; Noto, R. *Appl. Organomet. Chem.* **2014**, *28*, 234-238. Massaro, M.; Riela, S.; Cavallaro, G.; Gruttadauria, M.; Milioto, S.; Noto, R.; Lazzara, G. *J. Organomet. Chem.* **2014**, *749*, 410-415.
47. Massaro, M.; Colletti, C. G.; Buscemi, G.; Cataldo, S.; Guernelli, S.; Lazzara, G.; Liotta, L. F.; Parisi, F.; Pettignano, A.; Riela, S. *New J. Chem.* **2018**, *42*, 13938-13947.